

^{68}Ga -Labeled radiopharmaceuticals for pretargeted PET imaging; synthesis of ^{68}Ga -HBED-CC-tetrazines

Elina Honkaniemi

Master's Thesis

Supervisor Anu Airaksinen

Radiochemistry

Department of chemistry

University of Helsinki

Finland

September 2017



| | | | |
|--|--|---|--|
| Tiedekunta/Osasto Fakultet/Sektion – Faculty Faculty of science | | Laitos/Institution– Department Department of chemistry | |
| Tekijä/Författare – Author Elina Maria Honkaniemi | | | |
| Työn nimi / Arbetets titel – Title ⁶⁸ Ga-Labeled radiopharmaceuticals for pretargeted PET imaging; synthesis of ⁶⁸ Ga-HBED-CC-tetrazines | | | |
| Oppiaine /Läroämne – Subject Radiochemistry | | | |
| Työn laji/Arbetets art – Level Master's thesis | | Aika/Datum – Month and year September 2017 | Sivumäärä/ Sidoantal – Number of pages 75 |
| Tiivistelmä/Referat – Abstract <p>An extremely high demand of ⁶⁸Ga-radiotracers has ascended during the last decade in the field of nuclear medicine. ⁶⁸Ga is a positron emitting radionuclide which is widely used in positron emission tomography (PET) studies due to its short half-life of 68 minutes and good labeling properties. ⁶⁸Ga can be produced on site using ⁶⁸Ge/⁶⁸Ga-generator which makes it a viable option in comparison to the cyclotron-based PET isotopes such as ¹⁸F. Gallium's coordination chemistry demands it to be coordinated with a ligand for it to be stable enough to be introduced to target peptide. For that reason, chelating agents are commonly used to stabilize gallium, such as DOTA, NOTA or TRAP. Major of the chelators are bifunctional which means they can also bind to the target biomolecule such as peptide or antibody.</p> <p>Tetrazine molecule is widely used in bioorthogonal cycloaddition reactions in live cell labeling. Bioorthogonal reactions are used in pretargeting approach where first the unlabeled antibody is administered to localize the tumour and after that, small rapid-clearing radiolabeled compound is injected to attach to the antibody.</p> <p>In this work, bifunctional chelating agent HBED-CC was first coupled with tetrazine and after successful synthesis, the compound was labeled with ⁶⁸Ga. Aim of the study was to discover the potential of this compound to pass the cell membrane and to determine its properties. The synthesis of HBED-CC-tetrazine was successfully optimized with good yields in a range of 65-85 %. Different synthesis conditions were tested including temperature, reaction time and the choice of a coupling reagent. Optimized conditions for the synthesis of HBED-CC-tetrazine were 48 hours in room temperature using the coupling reagent HATU. Radiosynthesis of [⁶⁸Ga] Ga-HBED-CC-tetrazine was also optimized using different temperatures, reaction times and precursor amounts. All conditions resulted in good radiochemical yields. Optimized conditions for radiolabeling turned out to be in 85 degrees for 20 minutes which resulted in 97 % of radiochemical yield with over 98 % radiochemical purity. The properties of the labeled compound [⁶⁸Ga] Ga-HBED-CC-tetrazine were tested, such as lipophilicity and the stability of the compound in a presence of iron.</p> | | | |
| Avainsanat – Nyckelord – Keywords ⁶⁸ Ga, PET imaging, labeling, pretargeting | | | |
| Säilytyspaikka – Förvaringställe – Where deposited E-thesis | | | |
| Muita tietoja – Övriga uppgifter – Additional information | | | |

Contents

| | |
|---|----|
| Abbreviation list | 4 |
| 1. Introduction | 5 |
| 2. Positron emission tomography (PET) | 6 |
| 2.1. Principle | 7 |
| 2.2. Designing a new radiotracer for PET | 11 |
| 3. Pretargeting..... | 12 |
| 3.1. Bioorthogonal pretargeting | 16 |
| 3.1.1. Tetrazine..... | 21 |
| 4. Gallium-68..... | 23 |
| 4.1. Production of ^{68}Ga | 24 |
| 4.2. ^{68}Ga coordination chemistry..... | 25 |
| 4.3. Radiolabeling with ^{68}Ga | 26 |
| 4.4. Chelators for ^{68}Ga labeling..... | 26 |
| 4.4.1. HBED-CC | 30 |
| 5. Coupling reagents for amide bond formation | 31 |
| 6. Aim of the study..... | 34 |
| 7. Experimental part..... | 36 |
| 7.1. Materials | 36 |
| 7.1.1. Methods and instruments for analysis of the synthesis products | 36 |
| 7.1.1.1. High-performance liquid chromatography (HPLC) | 36 |
| 7.1.1.2. Mass spectrometry (MS) and nuclear magnetic resonance (NMR) | 38 |
| 7.1.1.3. Autoradiography | 39 |
| 7.1.2. $^{68}\text{Ge}/^{68}\text{Ga}$ -generator..... | 39 |
| 7.1.3. Chemicals | 40 |
| 7.2. Methods | 42 |
| 7.2.1. Synthesis of the precursor for radiolabeling | 42 |
| 7.2.1.1. Deprotection reaction | 46 |
| 7.2.2. Radiosynthesis of ^{68}Ga | 48 |
| 7.2.3. Determining the lipophilicity..... | 50 |
| 7.2.4. The Fe challenge experiment and the stability of the product 5b | 50 |
| 8. Results and discussion..... | 51 |
| 8.1. Optimizing the synthesis of the precursor for radiolabeling | 51 |
| 8.2. Radiolabeling with ^{68}Ga | 56 |
| 8.3. Determining the lipophilicity | 59 |

| | | |
|------|--|----|
| 8.4. | The Fe challenge experiment and the stability of the product 5b | 60 |
| 9. | Conclusions and future work | 61 |
| 10. | References..... | 63 |
| 11. | Appendix | 70 |

Abbreviation list

DFO = Desferrioxamine

DMF = Dimethylformamide

DOTA = 1,4,7,10 -Tetraazacyclododecane-1,4,7,10-tetraacetic acid

EDC = 3-(((ethylimino)methylene)amino)-N,N-dimethylpropan-1-amine

HATU = 1-[Bis(dimethylamino)methylene]-1H-1,2,3-triazolo[4,5-b] pyridine-1-ium 3-oxide hexafluorophosphate

HBED-CC = 3-(3-(((2-(tert-butoxy)-2-oxoethyl)(2-((2-(tert-butoxy)-2-oxoethyl)(5-(3-(tert-butoxy)-3-oxopropyl)-2-hydroxybenzyl)amino)ethyl)amino)methyl)-4-hydroxyphenyl)propanoic acid

HEPES = 2-[4-(2-hydroxyethyl)piperazin-1-yl]ethane sulfonic acid)

HPLC = High performance liquid chromatography

NOTA = 1,4,7-triazacyclononane-1,4,7-triacetic acid

PET = positron emission tomography

RCY = radiochemical yield

RT = room temperature

SOS = start of synthesis

SPECT = single-photon emission computed tomography

TLC = thin layer chromatography

TRAP = 3,3',3''-(((1,4,7-triazonane-1,4,7-triyl)tris(methylene))tris(hydroxyphosphoryl))tripropanoic acid

TSTU = N,N,N',N'-Tetramethyl-O-(N-succinimidyl)uronium tetrafluoroborate

1. Introduction

Positron emission tomography (PET) imaging is widely used and powerful non-invasive method in the field of nuclear medicine. It is highly sensitive imaging method that is commonly used in several applications such as oncology, neuroimaging and cardiology. PET imaging is a valuable tool in medical and diagnosis applications, but also for research purposes for instance in drug discovery.

In PET imaging process, tracer containing radioactive substance is injected to human body. PET uses positron emitting radionuclides, such as ^{11}C , ^{18}F , ^{13}N , ^{15}O and ^{68}Ga . ^{18}F has long been the most used nuclide, but nowadays ^{68}Ga is becoming more relevant due to easy access from generator and its good radiolabeling properties. When these positron emitting radionuclides decay, a positron is emitted. As the positively charged positron confronts negatively charged electron, annihilation process occurs ejecting two 511 keV gamma rays that can be detected in the PET system.

New techniques for PET imaging are constantly being developed. One major challenge in PET imaging has been the specific delivery of radioactive compound. Monoclonal antibodies (mAbs) have long been used as a vector for radionuclide targeting for tumor detection and imaging. However, antibodies are large molecules that diffuse and transport slowly in the body. Even though antibodies reach the tumor cell relatively fast, their complete binding to it can take days due to slow pharmacokinetics. Thus, tracers with longer half-lives are needed. This leads to poor target to background ratios and to higher activity doses to healthy cells.

Therefore, a method called pretargeting was invented to solve this problem. In pretargeting imaging, an unlabeled antibody is first administrated in to body and left to locate its target cell such as cancer. After this step, small labeled molecule is injected to locate antibody and bind to it. Due to its small size, any excess of labeled molecule clears rapidly from blood. For this reason, pretargeting method provides better target-background ratio and therefore better images in PET imaging. Several different pretargeting methods have been reported so far and it has been proven that this approach has brought an excellent contribution to the area of PET imaging.

The choice of radionuclide is important as their properties and especially radiolabeling conditions may differ quite a lot. Radiometals such as ^{68}Ga need a chelating agent to be able to bind to antibody. As chelating agent's properties and affinities towards radiometals differ significantly, it also needs to be chosen carefully. Affinity to radiometal must be high enough to prevent any metal exchange in human body.

This master's thesis focuses on development of a synthesis method for HBED-CC-tetrazines, which are precursors for two new tracer candidates for pretargeted imaging, and on development of a radiolabeling method for HBED-CC-tetrazines with a positron emitting ^{68}Ga . Chelating agent HBED-CC is used to bind ^{68}Ga forming coordination complex. Tetrazine part is widely used in pretargeting purposes in fast occurring bioorthogonal click reactions.

Radiolabeled product [^{68}Ga] Ga-HBED-CC-tetrazine **5b**, was tested for different properties, such as lipophilicity and stability to estimate the compounds suitability as a PET imaging tracer.

2. Positron emission tomography (PET)

Positron emission tomography, also called PET imaging, is a nuclear medicine imaging method. It is a powerful method that is commonly used in *in vivo* biodistribution studies of molecular probes labelled with radioactive positron emitting nuclide (Phelps et al.,1975).

PET has several applications for example detecting cancer and determining whether the cancer has spread in the body, brain disorders, heart problems etc. Computed tomography (CT) and magnetic resonance imaging (MRI) are other commonly used imaging methods and they can provide excellent structural information about diseased organs. However, they provide relevant information only when the disease has already altered the anatomy by chemical changes. PET imaging occurs in a molecular level which makes it an excellent tool for detecting ongoing disease process.

Most commonly used radiotracers are ^{11}C , ^{15}O , ^{13}N and ^{18}F , among ^{68}Ga . They are all positron-emitters with relatively short half-lives. Short half-life is needed to minimize the radiation hazards to the patient. Radionuclide has to be attached to a probe that has the ability

to bind to a target molecule in patient. The target molecule can be for example a cancer cell or some other human tissue. Radiolabeled compound is then administrated to the patient where the compound binds to the target molecule. The distribution of the radiolabeled compound can then be detected using the imaging process with PET scanner.

PET imaging has a better resolution and sensitivity compared to for example single-photon emission computed tomography (SPECT) imaging. SPECT imaging is another imaging method for biomedical applications.

However, PET imaging has also some drawbacks. Compared to CT or MRI, the results with PET imaging are not so anatomically exact because PET gives information only from the cells the radioactive molecule has bonded. This means that it can be difficult to localize the accumulation without a method that can give anatomic information about the exact location. Therefore, combined imaging modality of PET/CT system is usually used.

2.1. Principle

PET imaging is based on injecting tracer compound labeled with positron emitting radionuclide and detecting the annihilation coincidence (Zanzonico et al.,2004). When a positron emitting radionuclide decays, it emits a positively charged particle, a positron. As positron moves along, it confronts an electron which has a negative charge opposite to positron. The confront produces annihilation pair consisting two photons travelling to opposite directions. PET imaging is based on detecting these photons in the scintillator of the scanning device. The principle of annihilation and detection of the photons is pictured in figure 1.

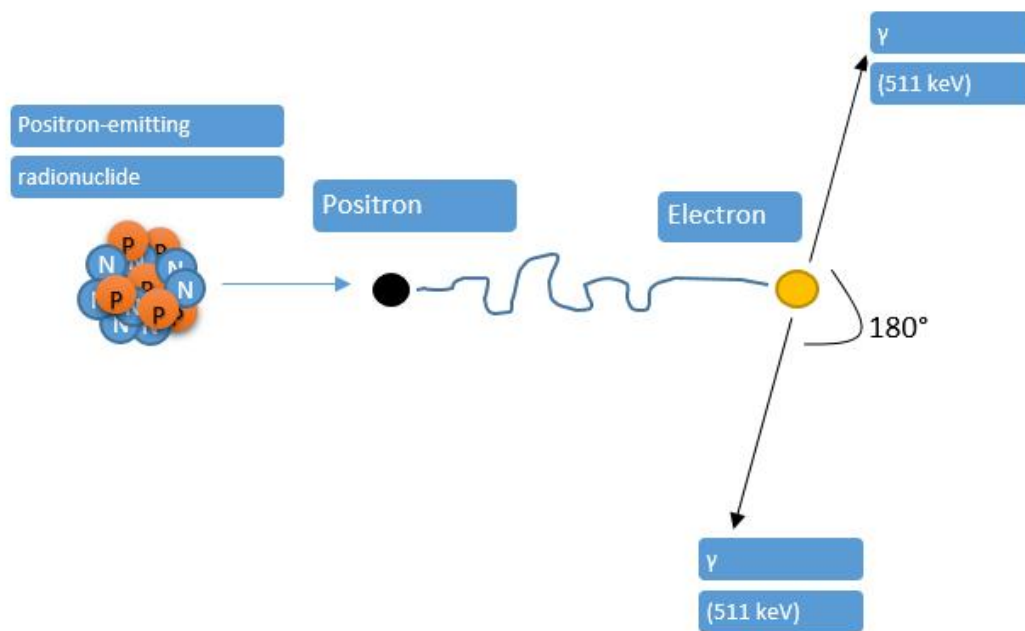


Figure 1. The decay of positron emitting radionuclide and the annihilation process.

PET scanner consists of multiple scintillation detectors around the scanner's circular shape. When the photons with an energy of 511 keV smash into the scintillation crystal, they get absorbed to the crystal lattice generating a light photon as a response (Vallabhajosula et al., 2009). Produced light photon creates then an electronic pulse in the multiplier. From multiplier, photons move to amplifier where they get strengthened. After this, electronic pulse can be detected and processed in a computer.

Detector crystal material can differ in PET systems. Bismuth germinate oxide (BGO), cerium doped lutetium oxyorthosilicate (LSO) and cerium doped gadolinium oxyorthosilicate (GSO) have been known to be used in PET detectors (Schöder et al., 2003). Detector has to have a high stopping power to ensure that all 511 keV photons are noted and absorbed (Del Guerra et al. 2004). Other requirements for ideal detector are high energy, spatial and timing resolution.

When detectors are processing the signal from the source, a time interval occurs while an acceptance of a new signal is not possible (Ziegler,2005). This time interval is called dead-time loss. During this time the crystal is not able to process a new signal and it will be lost.

If the counting rate is high, the effect of dead-time loss can affect greatly the amount of signals achieving the crystal.

The imaging method is based on the detection of the two annihilation photons emitting at 180° angle at the same time on opposite sides of the scanner. This process is based on annihilation coincidence detection (ACD). ACD enables to establish the line of response (LOR) which assists to locate the source of the annihilation pair in the patient. LOR is a line between two detectors which displays a possible path of emission. Annihilation pair must hit the opposite detectors during a time interval of 12-15 ns in order to be considered to be in coincidence. The annihilation pairs that exceed the time limit fall out of range and are not detected.

Coincidence events have three different types; a true coincidence, a random coincidence and a scatter coincidence (figure 2.) (Bolus et al., 2009). A true coincidence happens when two photons from annihilation exceed the material without interaction and achieve the detectors. A random coincidence is an event that happens when two photons from different annihilation processes reach the opposite detectors at the same time. Finally, a scatter coincidence occurs when one or both of the photons scatter on their way because of interactions with material. Annihilation radiation can undergo Compton scattering which influences the photons to change their directions and form coincidences in wrong locations. When scattered photon travels through material, it loses some of its energy.

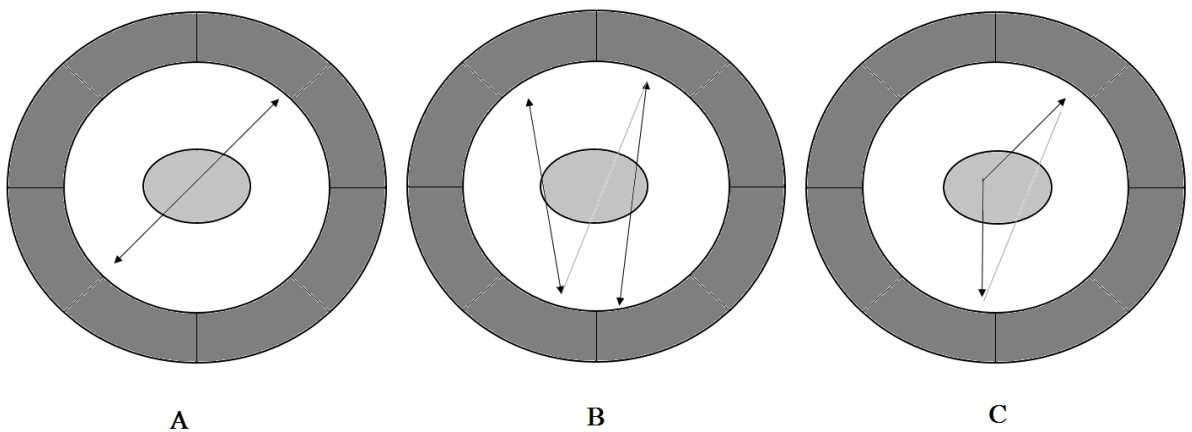


Figure 2. Coincidence events of PET imaging. True coincidence (A), random coincidence (B) and scattered coincidence (C). Figure is based on an article by Bolus (Bolus et al., 2009).

A random and a scatter coincidence are events that affect a true coincidence and therefore affect the image of PET scanner by increasing the background in the image. To decrease detection of false coincidences, some modifications have to take place. Scatter coincidence photons can be rejected using an energy threshold. Energy threshold is a window that can be appointed to let through only photons with an energy of 511 keV. Even though the energy window cuts out major part of scattering photons, some scattering radiation can still pass through.

As scattered photons are located to wrong LOR they are also removed from the right LOR when scattering (Lewellen, 2008). This phenomenon called attenuation affects PET image quality because of the loss of coincidence events. Photons interactions with different materials in patient can also attenuate the photon as it travels to the detectors. Together these effects can alter the photons ability to reach the detector within time and energy windows. To minimize the attenuation, some corrections are in order. Attenuation can be estimated using CT equipment together with PET. However, usually event though attenuation corrections are done for the image, still both the corrected and uncorrected images are read.

PET imaging is an excellent imaging method as it is highly sensitive compared to other imaging modalities. High sensitivity allows smaller tracer amounts which means radioactive substances can be injected in nano or pico molar quantities. One major potential for PET imaging is its excellent quantitativity. PET is able to measure the radioactivity that is injected without emphatically. Quantitative measurement especially with ^{18}F -FDG PET has become extremely useful tool in diagnosis in the area of oncology.

One of PETs good properties is that it allows the use of short half-life radionuclides. Most common used nuclides ^{11}C ($t_{1/2} = 20,3$ min), ^{15}O ($t_{1/2} = 2,03$ min), ^{13}N ($t_{1/2} = 9,97$ min), ^{18}F ($t_{1/2} = 109,8$ min) and ^{68}Ga ($t_{1/2} = 68$ min). This ensures lowest possible radiation doses to patients going through PET imaging. Most of these elements are found naturally and from human body. This allows relatively easy substitution mechanisms with element's stable form. Biologically stable compounds can also be modified to radiolabeled analogues in a way that their properties are enhanced for nuclear imaging (Abogye et al., 2003).

However, there are also some drawbacks in the use of PET imaging. PET system has a relatively low spatial resolution and it can only image biological disorders at the molecular level. Therefore, PET systems are usually connected to computed tomography (CT) forming hybrid PET/CT system. With this combined imaging modality, CT is not used just to acquire anatomical and functional images but it also corrects the attenuation of the PET data.

Other limitation is the price of PET systems. They can be quite expensive which can be a restrictive factor in acquisition intensions for research centres. Radionuclides short half-live can also be a challenging factor in laboratory scale. Radiolabeling conditions and procedures must be accomplished quickly and readily on-site of the PET imaging,

2.2. Designing a new radiotracer for PET

For a radiotracer to work efficiently as a PET imaging agent, it needs to fulfil several requirements. Development of a new PET imaging probe demand organic synthesis, radiolabeling conditions assessment both *in vitro* and *in vivo*, and kinetic modeling of the radiolabeled compound (Li et al., 2010). Molecular imaging probe can be a receptor, analogue, protein, antibody etc., as long as it is able to bind the radionuclide and form a stable compound or complex with it. Probe must also handle physical conditions and different biological reactions, such as metabolism and blood circulation.

Suitable radionuclide is added to the probe in a radiolabeling process. Radiolabeling procedure must be designed carefully and especially time consumption of the whole process is a critical step. No more than two times half-life of radionuclide should be spent for the whole procedure starting from the radiosynthesis and ending in the injection of radiotracer to patient. Therefore, synthesis must be fast and preferably suitable for automation in synthesis units. Synthesis should be optimized so that the radiochemical yield is high, radiochemical purity is sufficient and the specific activity is high enough.

Choice of the probe affects properties of the radiotracer greatly. Radiotracer should have quite small molecular weight for small molecules can clear from blood circulation faster. Small compounds also usually provide better target/background ratios. Often probe is chosen because of biological purposes. Radiotracer might be meant to target certain receptor and

then probe can be altered to resemble an existing ligand of this receptor. Radiotracers lipophilicity has also great value to its kinetics.

Another important value to consider with radiotracers is specific activity. Specific activity is defined by dividing the measured radioactivity per mass or mole of the unlabeled tracer that was injected (Bonardi et al., 2002). Specific activity tells about the ratio of radiolabeled tracer to the unlabeled probe. Specific activity should be high enough to provide good quality images but also low enough to prevent saturation of detectors. However, each radionuclide has maximum specific activity that can be calculated from the half-life and mass number of nuclide (Fowler et al., 2003).

As radiotracer is administered to human, it must possess favourable pharmacokinetics. Adsorption, distribution, metabolism and excretion (ADME) are constantly affecting radiotracer and in order to bind its target, radiotracer has to be modified to endure them. However, adsorption doesn't have that significant role because radiotracer is usually injected intravenously. Metabolism of radiotracer should be noted to make sure no harmful or toxic metabolites are decomposed in body. Formation of radioactive metabolites disturbs the PET imaging producing background.

3. Pretargeting

Monoclonal antibodies (mAbs) have increasingly been used as an efficient delivery aids for tumour targeting in imaging and therapeutic applications. Monoclonal antibodies are antibodies that can be altered to bind to admired substance. Therefore, they have high binding affinities and an excellent specificity for their target molecule such as different antigens on the cancer cell membrane. However, due to their big size mAbs tend to have slow diffusion to tissue and a clearance from blood circulation can take long which often leads to low target-to-background ratios. Smaller proteins and antibody fragments might have better clearance but thus their targeting ratio remains lower.

Pretargeting approach was first investigated in 1985 by Reardan *et al.* The research group was investigating radiochemistry chelates when they discovered the fact that small metal chelates could clear from the body a lot faster than bigger antibodies. This finding led to further studies and the concept of pretargeting was established.

Pretargeting method is particularly useful with large mAbs which usually have a slow tumour accumulation and retention. Pretargeting allows these antibodies to first contact the tumour cells before injecting the radioactive compound. This way the antibody can achieve maximum tumour uptake without causing redundant radiation. Pretargeting method allows the large mAbs to have high tumour affinity but at the same time have the good clearing properties of a smaller molecule.

Pretargeting concept was first conceived as a method to improve imaging by decreasing the background activity. Development of pretargeting strategies happened first at the radioimaging and radiotherapy of cancer area where it is crucial to have good difference between healthy and cancer cells.

The principle of pretargeting consists of a multi-step process where first the unlabelled antibody is administered to localize and bind to the tumour by its anti-tumour binding site. Antibody is then let to bind to the tumour and the excess of it left to circulate and clear from the blood. After this step, the small, rapid-clearing radiolabelled compound is then administered to attach to the sites which the antibody has accumulated. Any excess of small radiolabeled compound clears rapidly from the body. This radiolabeled compound must have a high affinity to the antibody. This can be achieved by carefully choosing and modifying the functionality groups of the antibody. The radiolabelled compound is administered only after the antibody has reached its destination and a major part of it has cleared from the blood circulation. Simplified pattern of pretargeting method is demonstrated in the figure 3.

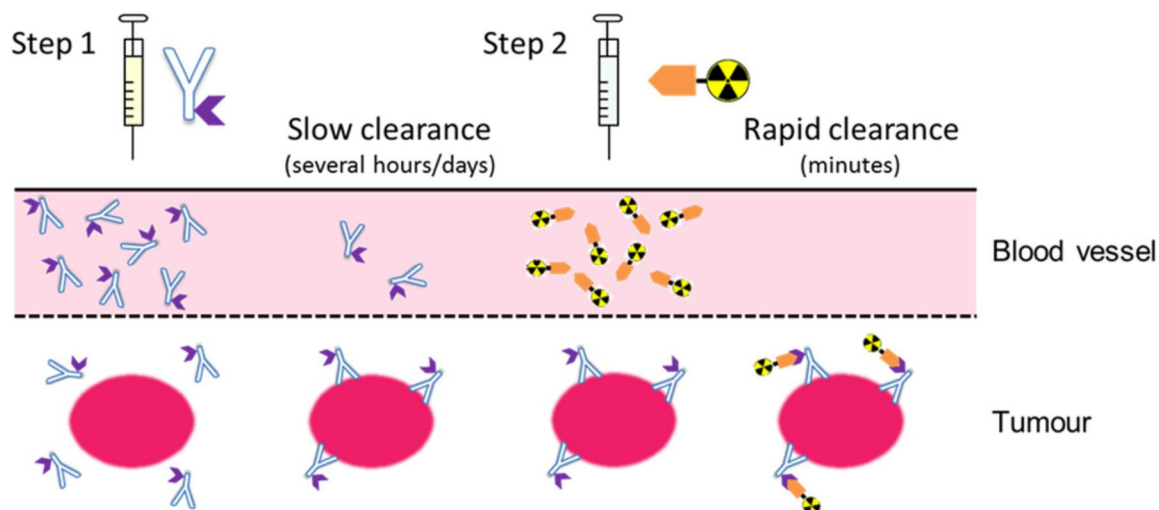


Figure 3. The basic idea of a two-step pretargeting method (Knight and Cornelisson, 2014). First the antibody is administrated to blood circulation following the injection of the radiolabelled compound with rapid clearance.

The radiolabeled compound is preferred to be small so it reaches the tumour quickly. The rapid clearance of the compound reduces the radiation exposure outside of the tumour. Small and fast clearing compound will also bind rapidly to the accumulated antibody and the rest unbound radiolabeled compound will clear fast from the blood circulation.

There are several different methods for achieving the pretargeting procedure. The original pretargeting approach was based on the idea of using bispecific antibodies which can bind to the target antigen as well as the radioactive metal-complex (Stickney et al., 1991). In the early days, ^{111}In was almost the only nuclide considered, but in further studies other nuclides have gained more visibility in the area.

However, this method had several drawbacks. The amount of bispecific antibody greatly affected the tumour uptake. If the injected dose was too low, the uptake remained quite low (Lollo et al., 1994). Also, if the injection time between bispecific antibody and hapten was too long, the tumour uptake would also remain too low. Conversely, if the amount of bispecific antibody was too high, and the delay between injections was short, the uptake would then be reasonable but the radioactive hapten would stay in the blood circulation elongated. For that reason, the pretargeting method had to be improved.

Another method for pretargeting is to use biotin and (strept) avidin (Hnatowitch et al., 1987). Avidin is glycosylated and positively charged protein that is found in the egg whites.

Streptavidin is a bacterial analogue of avidin and it has similar binding properties to biotin. Biotin is a vitamin which can be found from serum in low concentrations. Biotin has an extremely high affinity for avidin/streptavidin with a dissociation constant of $K_D=10^{-15}$ M (Green, 1963). This value exceeds the usual binding constants of antibodies for antigens which can 10^{-9} M be at highest (Chang et al., 2002). The bond forms very rapidly and has a good stability even in very high or low pH values. Biotin-(strept) avidin bond can also persist different organic solvents and denaturing agents which makes it relatively easy to handle. First studies in pretargeting exploited this strong binding constant of avidin-biotin. In these studies, first the biotinylated mAbs was administrated following the radioactive avidin injection (Paganelli et al., 1988). Labeled avidin then locates and rapidly binds the biotin that is attached to the tumour cell. The accumulation of radioactive avidin to biotinylated mAbs was demonstrated which led to further studies using this high binding pair. However, there are also some limitations to this method. Usually, radiolabeled streptavidin is injected after the antibody containing biotin. This may lead to higher activity doses if radiolabeled streptavidin binds to antibody-biotin compound that is still circulating in blood vascular system.

In some studies, avidin-antibody was injected first and after that the labeled biotin (Li et al., 2005). A three-step process was also demonstrated where first biotinylated antibody was injected, then excess of avidin was added and finally after that the labeled biotin could be injected. In all these methods, radioactivity in the tumour cell increased. However, injecting biotin-antibody first has also some disadvantages. Biotin occurs naturally in human cells, so in case of some tissue containing extra biotin, the background levels may rise too high for PET imaging.

Complementary oligonucleotides have also shown recently great promise as a pretargeting method. Complementary oligonucleotides, such as DNA as well as RNA, can form high affinity interactions with their complementary strands. DNA-DNA conjugation was studied by Bos et al. (Bos et al., 1994) in *in vitro* studies. In this study antibody-complementary DNA complex is administrated followed by radiolabeled complementary oligonucleotide. Results showed that this method might be useful for pretargeting purposes due to strong binding of DNA to antibody and good specific binding of oligonucleotides to cells.

Phosphordiamidate morpholino oligomers (MORFs) have been widely used in order to get decent signal amplification at the target (He et al., 2004). In this method, first the MORF

conjugated antibody is administered followed by a complementary MORF attached to polymer. Finally, radiolabeled MORF can be injected to locate the antibody in target cell. This sort of method differs from conventional pretargeting methods by having one extra step in the process. From the use of oligomers, MORFs have shown biggest potential in pretargeting.

The use of complementary oligonucleotides has some advantages comparing to the biotin-avidin approach. For example, single strand DNA samples that were injected in high concentrations and continuously did not show significant toxicities.

3.1. Bioorthogonal pretargeting

Bioorthogonal pretargeting reactions have recently gained great interest due to their rapid and highly selective nature (Van Swieten et al., 2005). Bioorthogonal pretargeting reactions use the combination of chemistry and biology. These reactions do not interfere or disturb biological systems as compounds used in bioorthogonal reactions only bind to those functional groups of molecules they are intended to. Binding of the molecules happens covalently which makes the formed product relatively stable. There are some requirements for the compounds participating in bioorthogonal reactions. Their functional groups must be modified so that they only interact with each other's and *in vivo* studies they should be nontoxic to the biological system.

These kinds of reactions are nowadays routinely utilized for applications in living systems. Like the pretargeting method, bioorthogonal reactions also consist of two steps. First the small molecule such as metabolic substrate or enzyme inhibitor attached with a bioorthogonal function group is administered to biological system. Once molecule has reached and bind to its target,

So far, a few different bioorthogonal reactions have been reported, such as the Staudinger ligation, [3+2] cycloaddition click chemistry reaction between alkynes and azides and [4+2] Diels-Alder cycloadditions.

Staudinger ligation was one of the first bioorthogonal reactions reported to occur in living systems (Saxon et al., 2000). Staudinger ligation is based on Staudinger reaction that has

been widely used in reactions converting azides into amines (Staudinger and Meyer, 1919). Reaction is based on using azide and phosphine in a production of azaphosphonire which can then be hydrolysed into amine and very stable phosphine oxide. Staudinger ligation is a modification of this reaction. Instead of hydrolysing the intermediate azaphosphonire, it is trapped intramolecularly in a way that it is capable of being stable in aqueous solutions and not to be hydrolysed. This can be done using ester or other compound containing electrophilic carbonyl. Reaction takes advantage of selective acylation of α -nitrogen of the intermediate. Staudinger ligations amide bond formation in aqueous solutions makes it highly compatible in biological systems. Azide acts as a soft nucleophile when most of the biological nucleophiles are hard. A simplified reaction of Staudinger ligation in bioorthogonal chemistry is demonstrated in figure 4.

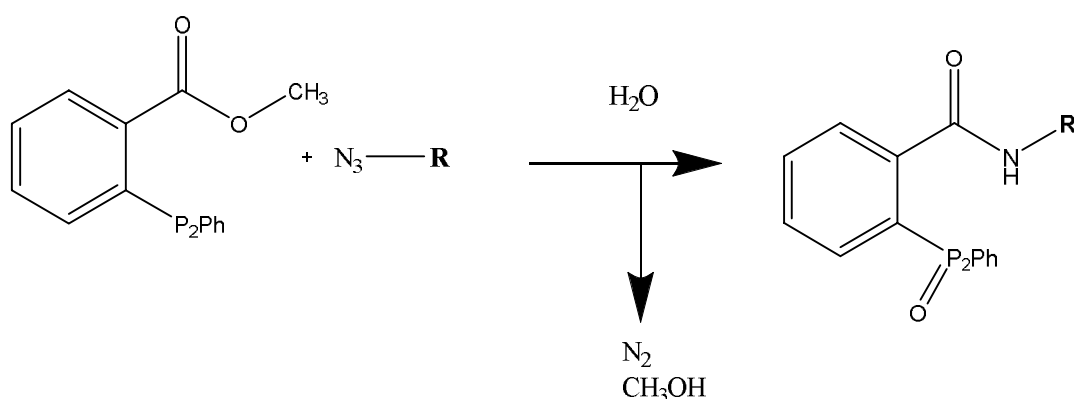


Figure 4. Simplified bioorthogonal Staudinger ligation between azide and triarylphosphine reagent. Group **R** marks for protein, biomolecule etc.

Staudinger ligation was later improved to a reaction called traceless Staudinger ligation. In this reaction, a cleavable linkage was added to the place of methoxycarbonyl. This method has been used in synthesis of heterobifunctional linkers for labeling with radiometals (Heldt et al., 2013). Traceless Staudinger ligation leaves the phosphine oxide as a separate by-product instead of it being as a part of the final product.

Both traced and traceless Staudinger reactions are highly selective and relatively easy to proceed. Furthermore, azides are small sized which makes them ideal for pretargeting purposes. Phosphines however are quite bulky molecules. In traced Staudinger ligation reactions, phosphine oxide group stays in the molecule. However, this bulkiness can be

decreased by adding polyethyleneglycol (PEG) chain. This is only necessary if phosphine group is attached to the labeled molecule that is injected later. If labeled molecule with phosphine group without addition of hydrophilic group is administered, binding of the molecule is not particularly selective towards the target molecule.

Even though Staudinger ligation shows great promise as a fast and selective reaction, it has not been proved to operate well in *in vivo* studies (Vugts et al., 2011). Studies in mice showed that Staudinger ligation had too slow reaction kinetics for pretargeting purposes. Ligation was demonstrated to reduce significantly and by-products were observed. Staudinger ligation's slow kinetics remain a problem in *in vivo* studies.

Recently, click reactions have gained wide interest in the area of biological labelling (Kolb et al., 2001). Click reactions are fast, high-yielding, relatively simple and they produce products that are stable at physiological conditions.

One relevant reaction in click chemistry is called strain promoted alkyne-azide cycloaddition (SPAAC) (figure 5). Its basic principle reaches out to copper catalysed [3+2] azide-alkyne Huisgen cycloaddition. However, SPAAC reaction can be proceeded without copper that can be harmful when injected to human body. SPAAC reaction involves biomolecule containing azide which then reacts with certain cyclooctene based probe. SPAAC reaction is highly efficient in complicated surroundings and in ambient temperatures and it has far better rate of reaction than Staudinger ligation.

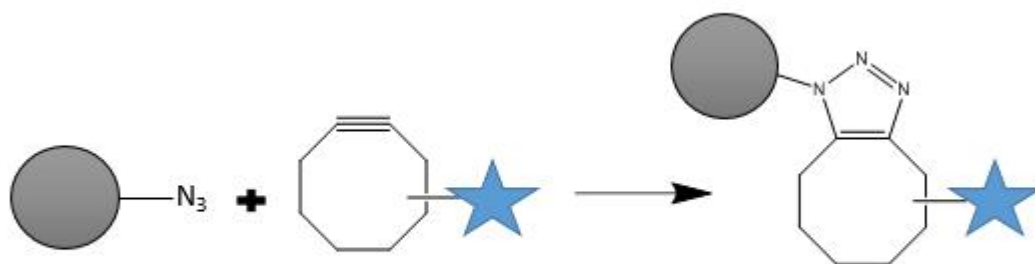


Figure 5. An example of strain promoted alkyne-azide cycloaddition (SPAAC) reaction.

SPAAC reaction has been investigated *in vivo* for pretargeting approach. Lee et al. reported SPAAC based bioorthogonal reaction in mice using mesoporous silica nanoparticles (MSNs)

that were processed with ^{18}F labeled azide compounds for PET imaging (Lee et al, 2013). In this study SPAAC reaction was accomplished successfully and PET imaging showed good results of radiotracer being accumulated to tumour location site. Biodistribution experiments were also tested *ex vivo* and results showed enhanced tumour-to-blood ratios.

Another bioorthogonal reaction approach using SPAAC reaction was tested using three different cyclooctene based probes and labeled them with ^{177}Lu (Van den Bosch et al.,2013). Even though *in vitro* stability test showed great promise, *in vivo* studies in healthy mice showed biodistribution and blood clearance to not be that efficient. These studies showed that SPAAC reaction has potential for bioorthogonal reactions in pretargeting approach even though it needs more research.

One recent development in the bioorthogonal chemistry is the use of tetrazines and strained alkene dienophiles in a reaction called inverse Electron-Demand [4+2] Diels-Alder (IEDDA) cycloaddition (figure 8). IEDDA reaction was first published in 2008 when Blackman et al. revealed the reaction between tetrazine(Tz) and trans-cyclooctene(TCO) forming pyridazines (Blackman et al., 2008). IEDDA is a fast, selective, high-yielding and clean reaction consisting of two steps. It doesn't need catalyst and the reaction can occur also in aqueous conditions. IEDDA reaction has been widely used with radiometals but also ^{18}F is known to be used (Reiner et al., 2014). Copper free IEDDA reaction works relatively well for metals as well as there is no competition with copper of chelator.

Unlike other bioorthogonal reactions in pretargeting, IEDDA has proved to show great promise also in *in vivo* pretargeting studies. Several studies have reported IEDDA based pretargeting approaches (Rossin et al., 2010, Zeglis et al., 2013, Devaraj et al., 2012). All these studies report similar approach to the issue. First antibody attached with TCO is administrated and let to locate its target cell. Then any excess of it is let to slowly clear from blood circulation. After this small rapidly clearing radiolabeled tetrazine is injected to locate antibody. When labeled tetrazine locates TCO-antibody, IEDDA reaction occurs fast followed by clearance of any excess of radioligand. Basic idea of IEDDA bioorthogonal approach is presented in figure 6.

Chemically IEDDA reaction consists of two steps. First tetrazine and trans-cyclooctene go through cycloaddition and they produce tricyclic species with a dinitrogen bridge. After this, dinitrogen is released and dihydropyridazine can be formed as a stable product (Devaraj et al., 2009).

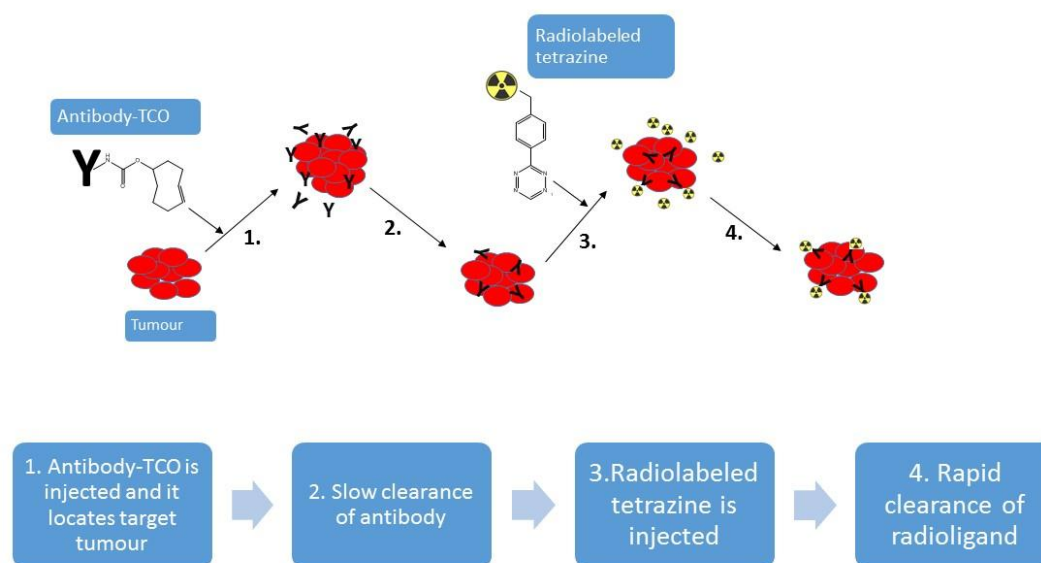


Figure 6. Basic principle of IEDDA reaction of trans-cyclooctene and tetrazine *in vivo* in pretargeting approach.

IEDDA reaction between tetrazine-DOTA and trans-cyclooctene-conjugated antibody was successfully demonstrated in mice for non-invasive imaging (Rossin et al., 2010). This study managed to establish that a reaction between two separate exogenous compounds can lead to high-yielding reaction in live mice bearing colon cancer xenografts. Antigen TAG72, which occurs in variety of cancer cell lines, was chosen for its strong binding properties. Anti-TAG72 antibody, CC49, was conjugated with TCO and tetrazine was bound to DOTA chelating agent. Bioorthogonal reaction was demonstrated to occur *in vitro* with a second order reaction rate constant of $13,090 \pm 80$ 1/Ms. Rapid bioorthogonal reaction was demonstrated to happen also in *in vivo* conditions and target to background ratios were observed to be reasonable.

In another study, $^{111}\text{InTz}$ -DOTA compound and TCO labeled antibody were administrated to mice and imaged with PET (Zeglis et al., 2013). This method was proved to be very efficient in delineating colorectal cancer xenograft in mouse.

Different approach was made by Devaraj et al. as they used dextran derivatives in ^{18}F labeled polymer-tetrazine compounds (Devaraj et al., 2012). Dextrans are widely used in *in vivo*

studies and therefore have suitable reaction kinetics. After modelling of reaction kinetics of TCO/Tz reaction, research group were able to predict ideal conditions and doses of two starting materials for *in vivo* use.

IEDDA reaction was used in a novel way by research group of Hou et al (Hou et al., 2016). Instead of using the regular TCO immunoconjugates, they synthesized supramolecular nanoparticles that were modified with TCO. Supramolecular nanoparticles are excellent for pretargeting purposes as they are highly small and therefore fast clearing from human body. Nanoparticles were administrated to tumour carrying mice followed by injection of tetrazine labeled with ^{64}Cu . This method showed strong PET imaging signals in the tumour area but also some radioactivity was noticed in liver. This might have been due transchelation of ^{64}Cu and could be avoided using ^{18}F .

Stability of TCO was greatly improved in *in vivo* conditions after a discovery that isomerization of trans-cyclooctene into unreactive cis-cyclooctene (CCO) deactivates TCO (Rossin et al., 2013). Isomerization was noted to happen because of interactions with copper-containing proteins. The issue was solved by inducing steric hindrance in the TCO molecule. The research group also discovered that TCO derivatives substituted with in axial position showed higher reactivity compared to equatorial positions. This lead to a much more stable and reactive compound as well as better tumour-to-non-tumour ratios. This was demonstrated in ^{111}In radiolabeling studies, where the radioactivity of tumour didn't show significant changes even after three days. This indicates for an extremely stable compound in *in vivo* conditions.

3.1.1. Tetrazine

Tetrazine has been widely used in bioorthogonal cycloaddition reactions in live cell labeling. Tetrazine ligations used in bioorthogonal reactions were first presented in 2008 in IEDDA reactions (Blackman et al., 2008). Basic structure of tetrazine compound is presented in figure 7. This basic structure consists of six-membered aromatic ring containing four nitrogen atoms although structure is often modified with different molecules since mere tetrazine is highly unstable.

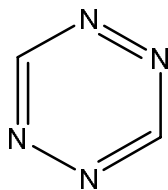


Figure 7. Structure of 1, 2, 4, 5-tetrazine.

In this master's thesis work, we used two different tetrazine derivatives with PEG4 link and an amine at the end of the link. The structures of tetrazine-PEG4-amines are presented in figure 8. Tetrazine compounds solubility to aqueous solutions is significantly improved by a hydrophilic polyethylene glycol PEG4 link. PEG link also decreases steric hindrance and reduces aggregation.

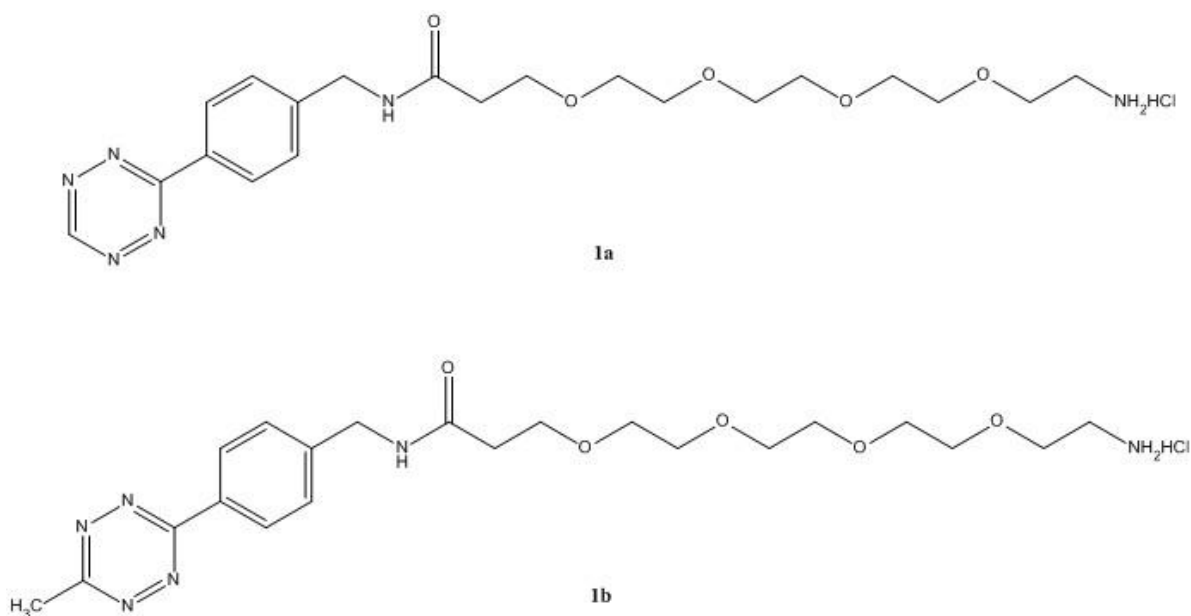


Figure 8. Structures of tetrazine-PEG4-amine **1a** and methyltetrazine-PEG4-amine **1b**.

Tetrazine compounds are known to be very reactive as dienes and therefore react rapidly and efficiently in IEDDA reactions (Boger et al., 1983). Tetrazines can react with a wide range of dienophiles or pyridazines forming only dinitrogen N_2 as a by-product.

Tetrazine has been widely used together with *trans*-cyclooctene (TCO) analogues mostly in IEDDA reactions (Maggi et al. 2016). Reaction between tetrazine and TCO happens extremely fast with a reaction rate of $210\text{-}30000\text{L mol}^{-1} \text{s}^{-1}$ (Devaraj et al., 2009) which

makes it extremely suitable for bioorthogonal reactions. Reaction of TCO and tetrazine is presented in figure 9.

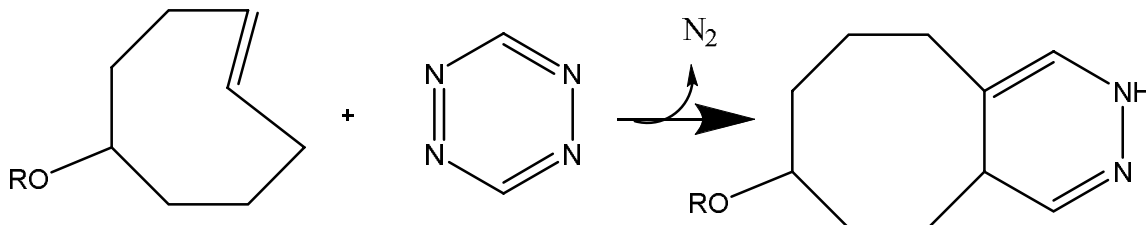


Figure 9. Reaction of TCO and tetrazine has an extremely high rate of reaction.

Chelating agent has to be used in order to use radiometal ⁶⁸Ga as an imaging agent in tetrazine structures. Because of ⁶⁸Ga coordination chemistry, it cannot bind directly to tetrazine. Pentetic acid (DTPA) have been used as an example as chelating agent with tetrazine (Nichols et al., 2014). In this work, amide bond is formed between the amine group of tetrazine-PEG4-amine and the carboxylic acid group of HBED-CC.

4. Gallium-68

Interest for ⁶⁸Ga radiopharmaceuticals in basic and in clinical study has increased rapidly over the past few years. ⁶⁸Ga has multiple advantages comparing to other radionuclides used in PET studies. ⁶⁸Ga is a positron emitter which decays with a half-life of 67, 7 minutes and it emits a high-energy positron (E= 1899 keV). It decays 89 % by positron emission and 11% via electron capture. Short half-life makes it compatible with pharmacokinetics of most of the low molecular weight radiopharmaceuticals such as peptides and antibody fragments. ⁶⁸Ga can be produced on site using ⁶⁸Ge/⁶⁸Ga-generator which makes it a viable option in comparison to the cyclotron-based PET isotopes such as ¹⁸F. The parent nuclide, ⁶⁸Ge has a long half-life of 270 days, which ensures the cost-effective availability of ⁶⁸Ga. Together with simple and short radiolabeling procedures, ⁶⁸Ga is a viable option for PET imaging.

4.1. Production of ^{68}Ga

As ^{68}Ga can be produced by $^{68}\text{Ge}/^{68}\text{Ga}$ -generator, it doesn't need on site cyclotron (Fani et al. 2008). The parent nuclide, ^{68}Ge decays with a half-life of 270.8 d by electron capture. The relatively long half-life of ^{68}Ge combined with the half-life of ^{68}Ga makes this pair nearly perfect for the generator system as the long half-life of ^{68}Ge allows the generator to have long a shelf-life. Consequently, the $^{68}\text{Ge}/^{68}\text{Ga}$ -generator can also be eluted several times a day for experiments.

The production of ^{68}Ge is demonstrated in the figure 10.

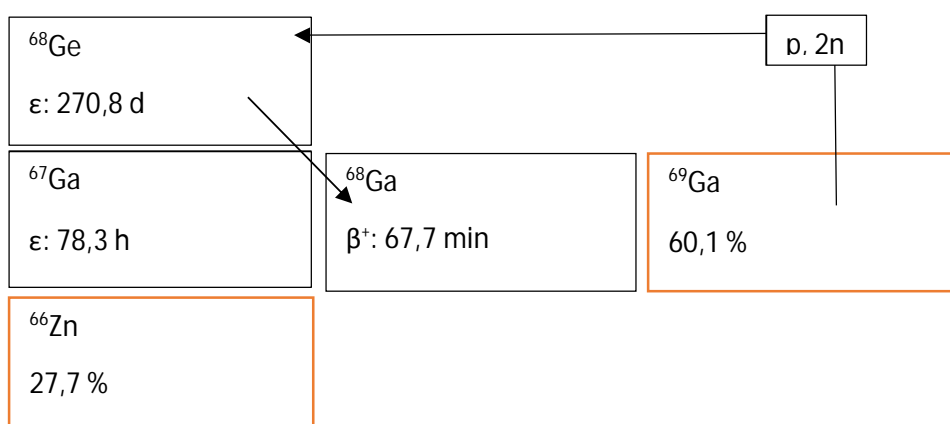


Figure 10. Production of ^{68}Ge by $(p, 2n)$ reaction from ^{69}Ge .

The first ^{68}Ga producing generators were eluted using EDTA so that the eluent could be directly used as a $[^{68}\text{Ga}]$ Ga-EDTA complex. However, since the complex was already formed, it did not leave room for the development of other ^{68}Ga complexes. Complex decomposition would have reduced the overall yield and been too time-consuming.

Generators were then developed to produce the ^{68}Ga as hydrated ionic form, $^{68}\text{Ga}^{3+}$. Different sorbent materials from metal containing Al_2O_3 or ZrO_2 to a bit better sorbent CeO_2 were tried but the yield of ^{68}Ga remained too low. Nowadays, the most common sorbent materials in generators are TiO_2 and SnO_2 for these kinds of generators provide good yields. ^{68}Ga must be separated from its parent nuclide ^{68}Ge to be used in coordination chemistry as ionic form. $^{68}\text{Ge}/^{68}\text{Ga}$ -generators operation is based on thin layer chromatography. The stationary phase is titanium dioxide in which the parent radionuclide ^{68}Ge is adsorbed. ^{68}Ge absorbs firmly to different solid supports, for example metal oxides such as Al_2O_3 , TiO_2 and

SnO₂. The mobile phase is a solvent able to elute ⁶⁸Ga from the system. The column is then placed inside a lead shield from where plastic eluate and eluent lines are provided. ⁶⁸Ga can be eluted from the column by ultrapure 0.1 M HCl using a syringe. The injection of HCl into the generator must be done carefully. Injection flow should be around 2 ml/min to avoid any extra pressure in the system. Air bubbles during the injection of the solvent must be avoided for they can also disturb the column.

⁶⁸Ge breakthrough from the generator must be eliminated for successful ⁶⁸Ga radiolabeling. Any usage of different metals must be avoided in elution of generator and possible metal impurities must be washed off from the generator.

4.2. ⁶⁸Ga coordination chemistry

Gallium has an electron configuration of [Ar] 4s² 3d¹⁰ 4p¹ which means it belongs to the group 3 in the periodic table. ⁶⁸Ga occurs mainly in the +3-oxidation state in aqueous solutions, due to its low redox potential. However, the free Ga³⁺ ion is only stable in acidic conditions. With higher pH, hydrolysis appears forming insoluble Ga(OH)₃. As the pH rises, gallium exits predominantly as gallate ion, Ga(OH)₄⁻ making it soluble in physiological pH (Green and Welch, 1989). However, the total solubility of gallium in physiological pH has a reliance on the specific activity of the compound.

The Ga³⁺ ion is classified as a hard acid, which means it will make thermodynamically stable complexes with highly ionic hard base ligand donors, such as hydroxamate, amine, phosphonate and carboxylic acids (Pearson, 1963). Therefore, gallium's chelate chemistry is being consisted of ligands containing nitrogen or oxygen donor atoms. Gallium's general coordination chemistry is very similar to transferrin, which occurs in physiological fluids (Bartholoma et al. 2012). Transferrin is a blood plasma glycoprotein containing Fe³⁺, which has a lot of same properties as Ga³⁺ ion. Both ions have almost the same ionic radii (62 pm for Ga³⁺ and 65 pm for Fe³⁺) and a lot of similarities in their coordination chemistry with a same major coordination number six. Therefore, especially the similarities in the coordination chemistry must be taken noticed in the preparation of gallium radiopharmaceuticals.

Ga (III) can form complexes with cyclic and open chain structures of polydentate ligands (Decristoforo et al. 2012). Ga (III) can form four-, five- and six-coordinated complexes but the six-coordinated complex is the most stable one.

4.3. Radiolabeling with ^{68}Ga

The radiolabeling with ^{68}Ga has to be performed in a pH range 3-4.5 (Nayak and Brechbiel, 2009). The adjustment of pH must be done rapidly after the elution of the generator to achieve efficient radiolabeling.

Different conditions for ^{68}Ga labeling of DOTA were attempted by Mokaleng et. al (2014). Labeling procedure included three different temperatures (room temperature, 60 °C and 100 °C) and different time intervals of 5-45 minutes. Labeling done in room temperature led to maximum 40 % labeling efficiency regardless of labeling time. With higher temperature 60 °C, labeling efficiency rose up to 83 %. Labeling time didn't seem to have much of an effect. With highest temperature of 100 °C, they were able to rise the labeling efficiency to 96 %. Labeling efficiency was demonstrated to vary between 86 to 93 % depending on labeling time. Effect of pH was also tested and the optimum was founded in between pH of 3-3.5.

4.4. Chelators for ^{68}Ga labeling

Since gallium can form insoluble hydroxide, $\text{Ga}(\text{OH})_3$, in water at physiological pH, direct radiolabeling of peptides or other similar compounds is almost impossible. For that reason, chelating agents are commonly used in order to stabilize gallium. Chelators must be kinetically inert in the pH 4-8 in clinical use so ligand transfer doesn't occur with transferrin protein. If ligand transfer with transferrin would happen, metal retention to liver and lung would be inevitable. Other properties for good chelator are ability to form peptide bond and also good solvent solubility.

Chelating agents are compounds that contain one or more ligands, which means they donate a lone pair of electrons in order to form a bond with metal ion. Almost all the chelating agents coordinate Ga with hexadentate structure, corresponding to gallium's six-coordinated

complex being the most stable one, although some chelators with coordination number four or five have been reported. Chelators must have multiple oxygen donor atoms and amines in order to bond ^{68}Ga strongly in pseudo-octahedral geometry. Most of the chelators are bifunctional, which means the chelator, that is complexing ^{68}Ga , can also bind to the target biomolecule for example antibody or peptide with a suitable functional group. Bifunctional chelator must fulfill two requirements; it should be kinetically stable so the bond between metal and chelate doesn't break even in the presence of other serum cations such as Ca^{2+} , Mg^{2+} or Zn^{2+} and also the chelation to metal should occur fast and efficiently due to the short half-life of Ga^{68} .

Desferrioxamine-B (DFO) was one of the first used chelators for radiolabeling studies with ^{68}Ga . It has been widely used in labeling with high radiochemical yield (Mathias et al., 1996). DFO binds gallium rapidly and with an excellent radiochemical yield. DFO consists of three hydroxamate groups that are available for coordination with Ga^{3+} (Figure 11). It also has free amine groups that can bind to biomolecules which makes it a bifunctional chelator. However, DFO can only bind metals in high concentration to ensure acceptable radiochemical yield (Caraco et al., 1998). When DFO was used in nanomolar amounts, Ga^{3+} coordination was not that effective and yield were noticed to be too low.

The most used chelator for radiolabelling with ^{68}Ga is currently the aminocarboxylate macrocycle DOTA, although also smaller NOTA is constantly used for its extremely stable complex with ^{68}Ga (Ray Banerjee et al., 2016). Recently, the triazacyclononane-phosphinate (TRAP) has also shown excellent binding ability for ^{68}Ga (Notni et al. 2011). The structures of DFO, DOTA, NOTA and TRAP are presented in the figure 11.

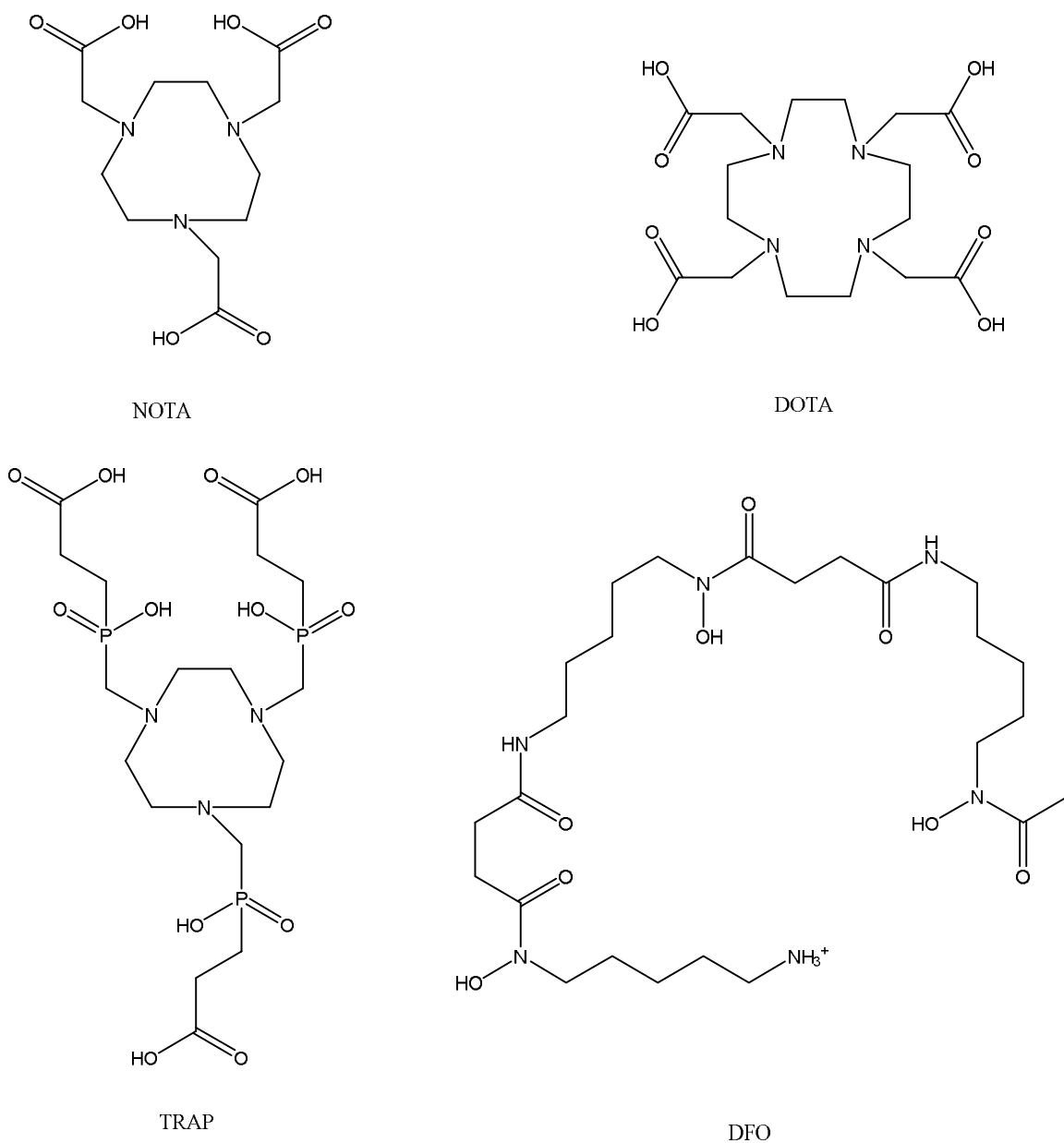


Figure 11. Structures of DOTA, NOTA and TRAP chelating agents for Ga⁶⁸.

DOTA chelator has been widely used in radiolabeling with ⁶⁸Ga for its structure and properties as a chelating reagent. DOTA radiolabeling with ⁶⁸Ga requires high temperatures from 90°C to 100 °C and relatively long incubation times (Wadas et al., 2010). This is because the ring distortion determines the reaction conditions. Compared to NOTA structure, DOTA has an extra carboxylic acid after complex formation which doesn't affect its properties as a bifunctional chelator.

DOTA's bioconjugate DOTANOC is a somatostatin analogue used clinically as a somatostatin receptor PET tracer. DOTA bioconjugates have shown to have high stability in

serum. Although the ^{68}Ga -DOTA complex has a high kinetic stability, it also has several disadvantages. The radiolabelling process requires a high temperature and quite long radiolabelling time. Typical radiolabelling conditions necessitate heating to 95 degrees for up to 30 minutes at pH below 5 (Heppeler *et al.* 1999). High temperature as well as the low pH aren't suitable for proteins which might be used in molecular imaging. Also, the long radiolabelling time allows ^{68}Ga to decay.

NOTA chelators have shown great stability and fast incorporation of ^{68}Ga . Labeling process can happen in lower temperatures than with DOTA (Blom *et al.*, 2011).

TRAP ligand is a NOTA derivative with a high efficient $^{68}\text{Ga}^{3+}$ complexation (Notni *et al.*, 2010). TRAP complex with ^{68}Ga possesses a high thermodynamic stability with a value of $\log K = 26,24$. Radiolabeling is reported to succeed in lower pH than usually with other ^{68}Ga chelators (Šimeček *et al.*, 2012). Formation of ^{68}Ga -TRAP complex occurred even in very acidic conditions with a pH as low as 1 meaning that ^{68}Ga eluate could be used straight from generator after elution with 0.1 M HCl.

Three different phosphinate ligands methylphosphinic (TRAP-H), methyl(phenyl)phosphinic (TRAP-Ph) and methyl(hydroxymethyl)phosphinic acid (TRAP-OH) as well as comparative 1,4,7-triazacyclononane-1,4,7-triacetic acid (NOTA) were labeled with ^{68}Ga and the stability of these compounds were tested by using potentiometry (Notni *et al.*, 2012a). Thus, all TRAP ligands were found to stay stable in both acidic and alkaline conditions. Complex formation with ^{68}Ga was reported to happen faster than with conventional chelators such as DOTA derivatives. Labeling was also able to occur within a wide range of pH starting even from $\text{pH} < 2$.

Same research group studied TRAP chelators labeling properties when attached to peptides (Notni *et al.*, 2012b). TRAP-, NOTA- and DOTA-peptides were compared and reported from their specific activity. TRAP-peptide was observed to be able to form complex with ^{68}Ga with a much lower precursor amount (1 nmol) than NOTA- or DOTA-peptides. Radiolabeling process was observed to be highly efficient which permits the process to be possible for kit labeling procedure.

4.4.1. HBED-CC

Since ^{68}Ga chemistry and its use in the PET imaging have been a rising topic in the research, new chelators for the radiolabelling with ^{68}Ga has been developed. One of these chelators is HBED-CC, which is a bifunctional chelator showing great promise in the radiolabelling studies with ^{68}Ga . The structure of HBED-CC is demonstrated in the figure 12.

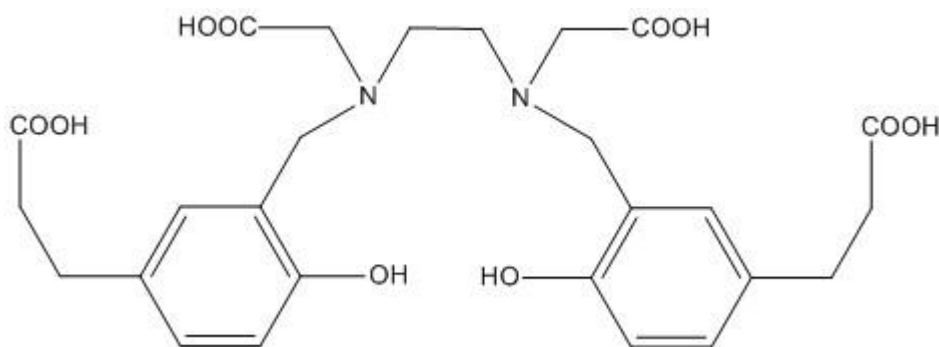


Figure 12. The structure of bifunctional chelator HBED-CC, which is used in the radiolabelling with ^{68}Ga .

HBED-CC consists of four carboxylic acids and two hydroxyl groups. Together with nitrogen, they form hexadentate complex with ^{68}Ga . Rapid ^{68}Ga complex formation with HBED-CC is allowed because of its acyclic structure (Eder et al. 2008). HBED-CC complex formation doesn't interfere with its bifunctionality as one carboxylic group does not participate in the ^{68}Ga -HBED-CC complex.

Compared to several other ^{68}Ga chelators, HBED-CC does not require a large amount of precursor for the radiolabeling to occur with a high yield. In a study of Eder et al. (2008) only 0.11 mg of HBED-CC-antibody (mAb425) complex was needed for an 89 % radiochemical yield with a specific activity of 37 GBq/ μmol .

The properties of HBED-CC in the radiolabeling with ^{68}Ga were investigated in a research by Eder *et al.* (2012) where they compared the [^{68}Ga] HBED-CC to DOTA complexes. They discovered that even though the lipophilicity of the DOTA complex is higher than HBED-

CC's, the structure of the molecule is crucial for better binding properties. HBED-CC's structure has an optimal aromatic feature because of the hydrophobic interactions.

Prostate-specific membrane antigen (PSMA) is a cell surface protein which PSMA is expressed normally in brains, kidney and prostate. Over-expression in prostate refers to prostate cancer. HBED-CC have been widely used as a chelator with Glu-urea-Lys(Ahx) PSMA inhibitor and it has been studied to be very good candidate for clinical applications of prostate cancer imaging (Eder et al., 2014).

HBED-CC can form diastereomers as it is forming coordination complex. This is due to the chirality of nitrogen atoms in its structure. However, it has been studied that the formation of diastereomers can be controlled (Eder et al., 2014). Applying different temperatures in the radiolabeling process, thermodynamically most stable diastereomer can be guided to form. When the radiolabeling was made in room temperature, it resulted in 50 % of another diastereomer to be formed. However, when sample was let to stay in room temperature in pH 4 for couple of hours, stereomer ratio quickly turned to thermodynamically more stable one. It was demonstrated that small amounts of less stable diastereomer in the sample did not significantly affect the binding properties of [⁶⁸Ga] Ga-PSMA-HBED-CC to PSMA.

5. Coupling reagents for amide bond formation

Coupling reaction between two starting materials HBED-CC and tetrazine-PEG4-amine was done by amide bond formation. Amide bond also known as peptide bond is a strong covalent bond that usually occurs between two amino acids in a peptide chain (Abdelmoty et al.1994).

To achieve the amide bond between carboxyl group and amino group, coupling reagent is to be introduced to the reaction. In this work, three different coupling reagents, TSTU, HATU and EDC, were used to compare their investment to the reaction. Each of the coupling reagents structure is presented in figure 13.

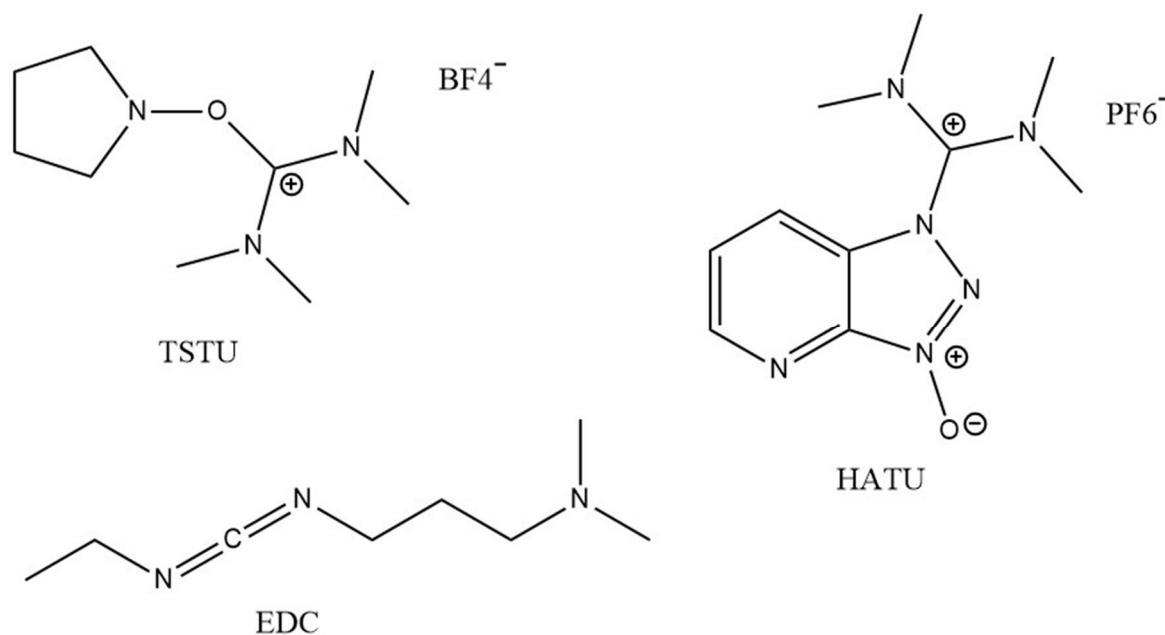


Figure 13. Coupling reagents used in the amide bond formation reaction.

All coupling reagents form the amide bond with the same principle (Montalbetti and Falque, 2005). The reaction consists of two steps, the activation of the carboxyl group and the acylation of the amino group. First step is the activation of carboxylic moiety. This step is usually the critical one and in order for it to work all other carboxylic acid groups need be protected to keep the reaction in control. If this step occurs too slowly, the next step might not happen due to coupling reagents degradation (Al-Warhi et al., 2012). In the second step, other compounds such as amino acids amine acts a nucleophile and attacks the activated carboxylic acid to form the amide bond. This step requires energy which explains why reacting carboxylic acid must be activated.

However, all three coupling reagents have little different properties and therefore the effect on the peptide formation reaction might differ (Han and Kim, 2004). TSTU is usually used in aqueous solutions. Formation of by-products must be taken noticed when working with TSTU. HATU is an aminium-based coupling reagent that is widely used for its good reaction yields and rates. It reacts rapidly producing very little side reactions and by-products. However, excess use of HATU can lead to unwanted reaction with unprotected N-terminal. EDC is a carbodiimide that is commonly used in the peptide modifying reactions. EDC can produce urea based side-product which can be disposed in the workup process.

Reaction with HATU usually happens in two steps. First HATU reacts with carboxylic acid forming the OAt activated ester. Then the activated ester reacts with amine the group. The reaction mechanism for the coupling reaction using HATU as a coupling reagent is presented in a figure 14.

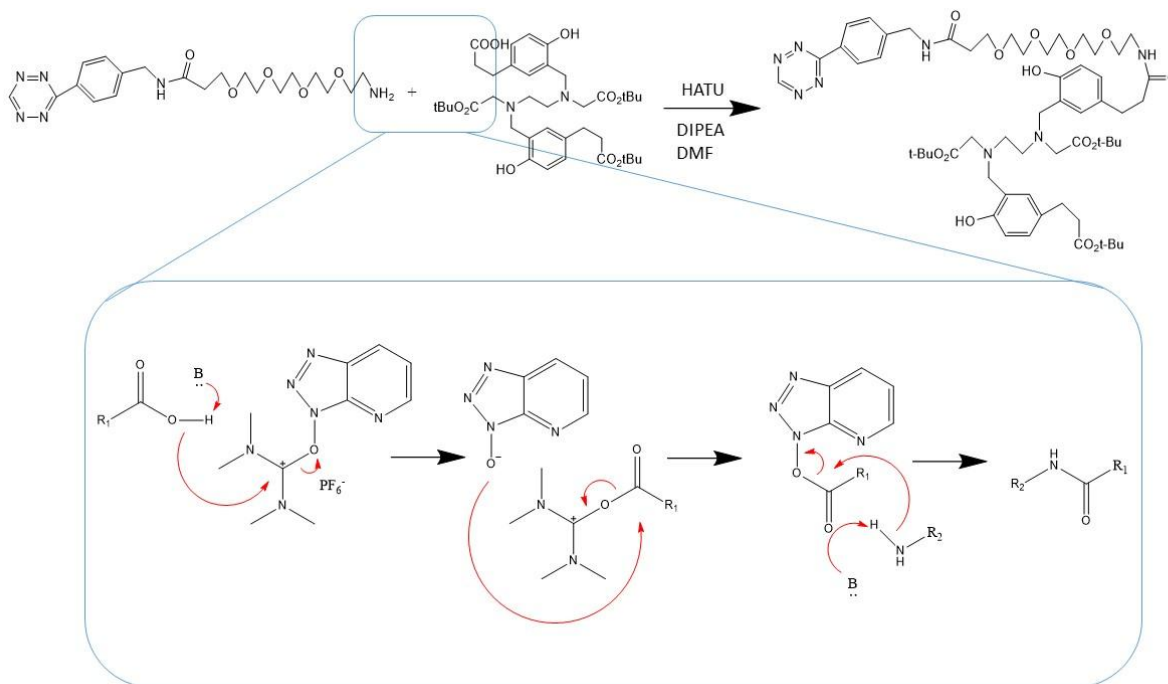


Figure 14. Reaction mechanism of coupling reaction with HATU.

Reaction starts as the base DIPEA deprotonates the carboxylic acid of HBED-CC. As a result, carboxylate anion forms and attacks the electron deficient carbon atom of HATU as seen in the figure 13. Derived carboxylic acid intermediate becomes activated and the formed HOAt anion can react with it in order to form OAt activated ester. After this, OAt activated ester reacts with tetrazine amine and the amide bond can form.

6. Aim of the study

The aim of this study was to develop tetrazine based compound labeled with ^{68}Ga that would have the possibility to cross the cell membrane. Ability to cross the cell membrane as well as the blood-brain-barrier can happen by passive diffusion, where the lipophilicity of a molecule plays a significant role. To achieve this aim, tetrazine was coupled with chelating agent HBED-CC so the labeling with ^{68}Ga could be possible. Coupling reaction as well as radiolabeling of the compound with ^{68}Ga was optimized with different conditions including different temperatures, reaction times and coupling reagents. The complete synthesis route is presented in figure 15.

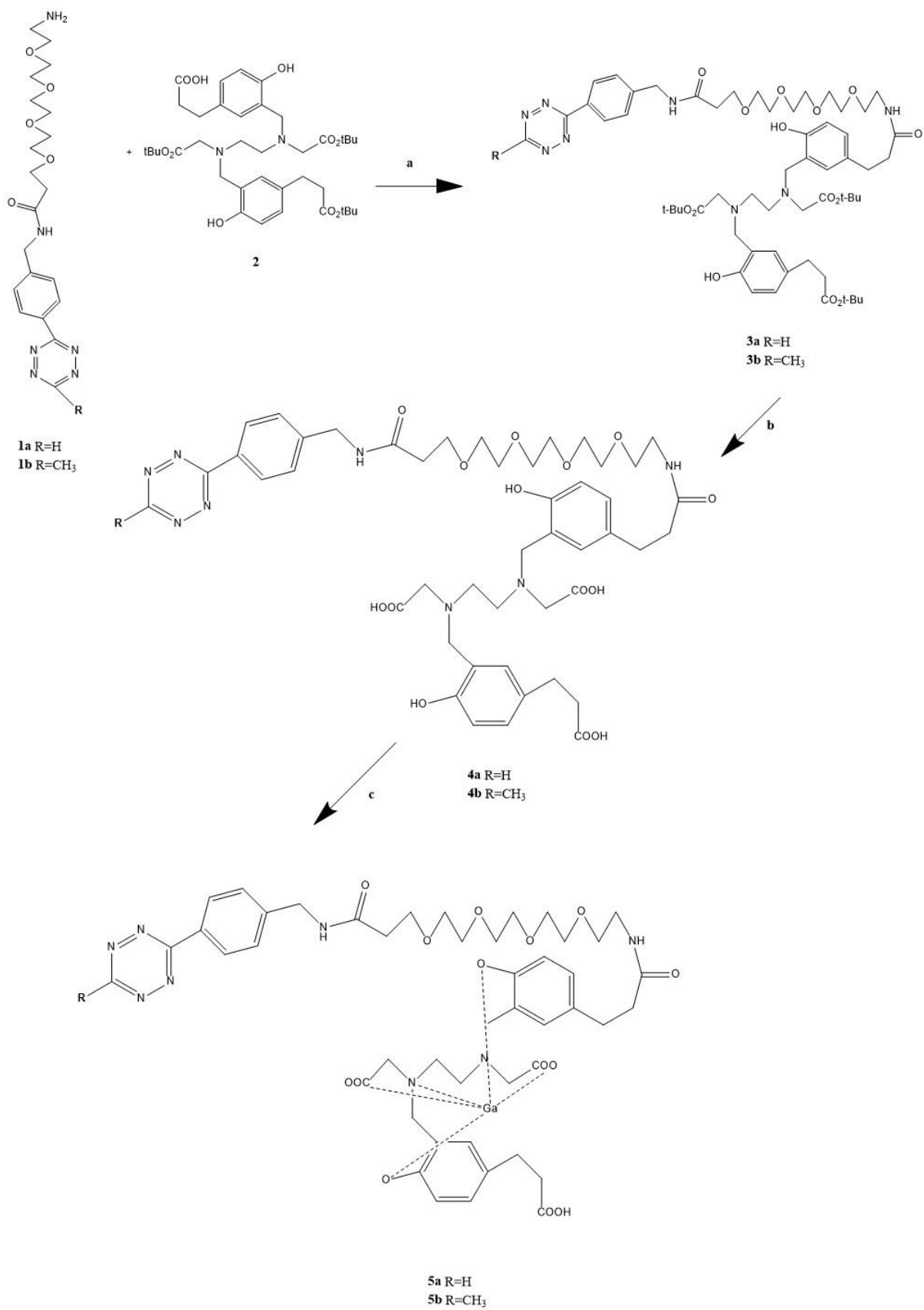


Figure 15. The synthesis route of the product. Reagents and conditions: a) HATU, DIPEA, DMF, 48 h, RT, dark, under argon b) TFA, DCM, 24 h, dark c) 1,5 M HEPES, 85 °, 20 min, pH 4.

7. Experimental part

7.1. Materials

7.1.1. Methods and instruments for analysis of the synthesis products

7.1.1.1. *High-performance liquid chromatography (HPLC)*

High-performance liquid chromatography (HPLC) was used for the purification of the product. HPLC is a technique that can be used for identification, quantification and purification of compounds. It is a type of liquid chromatography that uses high pressure for maximizing high speed and performance. Principle of HPLC relies on the mixture sample being divided into separated components based on its physical and chemical properties such as polarity, charge and molecular weight. HPLC consists of pumps, injector, column, detector and the computer data station. HPLC instrument is presented in figure 16.

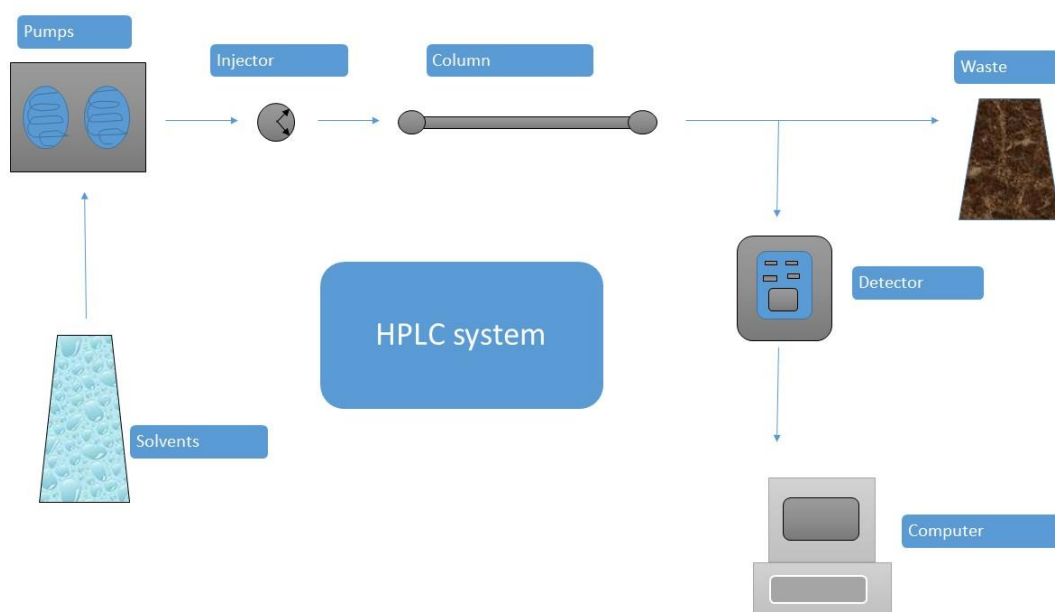


Figure 16. Simplified HPLC system.

The purpose of the pumps is to force liquid and the sample with it through the column and the whole system. Pressure in the system can alter plenty depending on the column size and flow rate. A typical pump can however reach pressure up to 500-600 bar. Pumps can function in isocratic or gradient mode. Isocratic pump keeps the mobile phase composition constant as the gradient pump can deliver multiple solvents and vary the mobile phase composition during the chromatogram.

Sample is injected to HPLC using an injector. Sample must be liquid and in a small volume. Injection can happen manually or automatically using an autosampler. Volume of the sample depends on the size of the column. From the injector, sample travels with continuously flowing mobile phase into the HPLC column.

Column is probably the most important part of the HPLC system. It contains the stationary phase in which the absorption of components takes place. Choice of the column is important in both analysis and purification processes. HPLC can be used as normal phase HPLC or reversed phase HPLC. In normal phase HPLC, stationary phase is polar and the mobile phase non-polar, such as hexane, chloroform or diethyl ether. Using this column type, more polar samples tend to stay in the polar surface of the stationary phase. Reversed phase HPLC is more commonly used method. In this method, stationary phase is nonpolar and mobile phase is more polar such as acetonitrile or water. This way compounds that are more polar tend to move with mobile phase and therefore have smaller retention times.

Detector is located at the end of the HPLC system and its purpose is to detect the analytes as they elute from the column. HPLC system can use a lot of different detectors depending on the examinee compound and its features. One of the most common detectors is ultraviolet-visible spectroscopic (UV/VIS) detector which uses compounds ability to show absorption spectrum of ultraviolet or visible light.

In this work, Shimadzu LC-solution equipment was used with CBM-20A control unit and LC-20AD pump. During the radiosynthesis, Canberra radiation detector was attached to the LC-system. Spectrums were analysed with a LC-solutions computer program.

7.1.1.2. *Mass spectrometry (MS) and nuclear magnetic resonance (NMR)*

For analysing the product, mass spectrometry (ESI-MS) and nuclear magnetic resonance (NMR) were used.

Mass spectrometry is a technique used to identify, detect and quantitate different compounds and molecules based on their mass-to-charge (m/z) ratio (Ho et al., 2003). MS instrument consists of ion source, mass analyser and detector. Mass spectrometers work by converting molecules of the analyte into charged ions using a certain ionisation process (De Hoffmann and Stroobant, 2007). ESI-MS uses electrospray ionisation source which uses a strong electric field to form an aerosol from the liquid sample. The liquid which contains the sample is passed through a capillary tube with a continuous stream that is generated by a high voltage. This high electric field induces a charge to pile up at the end of capillary tube causing the liquid to form little droplets with high charge. Because of N_2 gas flow or rising temperature in the system, droplets size decreases as the solvent in them evaporates. This leads to a surface charge density to increase and for the droplet radius to decrease. Finally, sample ions in the droplet are ready to desorb from the surface and continue to mass analyser to get analysed (Fenn et al. 1989). From the results, graph is given with corresponding peaks. The most intensive peak is assigned with abundance of 100 % and all the other peaks abundances are given as percentages of the biggest peak. In this work, a Bruker Daltonics microTOF-Q I (Bruker Daltonics, Bremen, Germany) was used and the data was analysed with DataAnalysis 3.2 software.

NMR is a commonly used technique for determining the structure of an organic compound (Bottomley, 1982). It advances magnetic properties of a certain atomic nuclei. The basic principle is that when magnetic nuclei is introduced into magnetic field, it will settle in a certain way with specific number of orientations (Gunther, 2013). Subatomic atoms, such as electrons, protons and neutrons have a spin. With some atoms, these spins are paired and cancelled by each other's, but others, such as 1H and ^{13}C the nucleus corresponds to overall spin. When atom confronts electric field, atom can transfer energy from basic energy level to higher energy level. This energy transfer corresponds to certain frequency that is the same frequency that energy is emitted when spin returns to its basic level. As the signal match, this transfer is measured and processed into a NMR spectrum. In this work, the NMR spectra

were recorded with Varian 300 MHz spectrometer and analyzed using the SpinWorks 2.4.2. software.

7.1.1.3. *Autoradiography*

Autoradiography was used in the determining of the radiochemical purity of the labeled compound. Autoradiography is technique to image radioactive emissions on a surface of an imaging plate. Photosensitive plate absorbs the radiation from radioactive sample and stores it on the plate that can later be read using a certain scanner. Plate consists of photo-stimulable phosphor that is coated on a polyester support layer (Johnston, 1990). Phosphor layer is usually bariumfluorobromide with a trace amount of bivalent europium (BaFBr:Eu²⁺). In the process, europium excites from ground state as Eu²⁺ to excited state as Eu³⁺. When plates are scanned with laser, excited BaFBr:Eu²⁺ crystals release energy as a blue light before returning to ground state. Blue light is collected in the system and image can be formed to computer. Autoradiography method is sensitive, relatively fast and has an excellent resolution. In this work, we used FLA-5100 scanner and Image Reader FLA-5000 Series V 1.0 computer program. Image was later processed with Aida Image Analyzer V 4.0 program. Autoradiography was used to read to the TLC plates during the radiolabeling process.

Radio-thin-layer-chromatography (TLC) scanner was used in determining of radiolabeling yields. Radio-TLC is a technique for analysing radiochemical purity from thin layer chromatography (TLC). With this technique, TLC is placed on the machine and the system proceeds the TLC providing a graph. High energy collimator and a bismuth germanate (BGO) detector are usually used for PET isotopes. In this work, Scan-RAM Radio-TLC detector (Lablogic) was used for the measuring and Laura software was used for analysing.

7.1.2. ⁶⁸Ge/ ⁶⁸Ga-generator

⁶⁸Ge/⁶⁸Ga-generators operation is based on column chromatography. The stationary phase is titanium dioxide in which the parent radionuclide ⁶⁸Ge is adsorbed. ⁶⁸Ge adsorbs firmly to different solid supports, for example metal oxides such as Al₂O₃, TiO₂ and SnO₂. The

mobile phase is a solvent able to elute ^{68}Ga from the system. The column is then placed inside a lead shield from where plastic eluate and eluent lines are provided.

$^{68}\text{Ge}/^{68}\text{Ga}$ -generator was Eckert-Ziegler model (batch HHGE01) with an original activity of 1850 MBq in 7.9.2015. For one elution generator could give approximately 200 MBq of ^{68}Ga per 10 millilitres of ultrapure 0.1 M HCl.

7.1.3. Chemicals

Starting materials, coupling reagents and other solutions are presented in table 1.

Table 1. Starting materials, coupling reagents and other solutions that were used in the work.

| Reagent | | Vendor |
|--|---|---------------|
| 3-(3-(((2-(tert-butoxy)-2-oxoethyl)(2-((2-(tert-butoxy)-2-oxoethyl)(5-(3-(tert-butoxy)-3-oxopropyl)-2-hydroxybenzyl)amino)ethyl)amino)methyl)-4-hydroxyphenyl)propanoic acid, (HBED-CC-tris(tBu)ester) | $\text{C}_{38}\text{H}_{56}\text{N}_2\text{O}_{10}$ | ABX |
| N-(4-(1,2,4,5-tetrazin-3-yl)benzyl)-1-amino-3,6,9,12-tetraoxapentadecan-15-amide hydrochloride, (Tetrazine-PEG4-amine) | $\text{C}_{20}\text{H}_{31}\text{ClN}_6\text{O}_5$ | Conju-Probe |
| 1-amino-N-(4-(6-methyl-1,2,4,5-tetrazin-3-yl)benzyl)-3,6,9,12-tetraoxapentadecan-15-amide hydrochloride, (Methyltetrazine-PEG4-amine) | $\text{C}_{21}\text{H}_{33}\text{ClN}_5\text{O}_5$ | Conju-Probe |
| 1-[Bis(dimethylamino)methylene]-1H-1,2,3-triazolo[4,5-b]pyridine-1-ium 3-oxide hexafluorophosphate, (HATU) | $\text{C}_{10}\text{H}_{15}\text{F}_6\text{N}_6\text{OP}$ | Sigma-Aldrich |
| 3-(((ethylimino)methylene)amino)-N,N-dimethylpropan-1-amine, (EDC) | $\text{C}_8\text{H}_{17}\text{N}_3$ | Sigma-Aldrich |

| | | |
|---|-----------------------|-----------------|
| N,N,N',N'-Tetramethyl-O-(N-succinimidyl)uronium tetrafluoroborate, (TSTU) | $C_9H_{16}BF_4N_3O_3$ | Sigma-Aldrich |
| Acetonitrile, (ACN) | CH_3CN | VWR |
| Deuterated Methanol | CD_3OD | C.E. Saclay |
| Dichloromethane, (DCM) | CH_2Cl_2 | Fisher Chemical |
| Dimethylformamide, (DMF) | C_3H_7NO | Sigma-Aldrich |
| Dipropylethylamine, (DIPEA) | $C_8H_{19}N$ | Sigma-Aldrich |
| Ethyl acetate | $C_4H_8O_2$ | Sigma-Aldrich |
| n-Hexane | C_6H_{14} | Merck |
| Methanol, (MeOH) | CH_3OH | Sigma-Aldrich |
| Tetrahydrofuran, (THF) | C_4H_8O | Sigma-Aldrich |
| Trifluoroacetic acid, (TFA) | $C_2HF_3O_2$ | Fisher Chemical |

Two buffers were used in the process. HEPES buffer (1.5 M, pH 7,5) was used in radiolabeling procedure and phosphate buffer (20 mM, pH 7.0) in the lipophilicity determination process. Both buffers were made in laboratory.

20 mM phosphate buffer was prepared by measuring 1.7 g of Na_2HPO_4 and 1.2 g of $NaH_2PO_4 \cdot 2H_2O$ and diluting to 1000 ml of water. After that pH was adjusted to 7.0 with NaOH.

1,5 M HEPES buffer was prepared by measuring 35.7 g of 4-(2-hydroxyethyl)-1-piperazineethanesulfonic acid and diluting it to 100 ml of milliQ-water. After that, pH was adjusted to 7.5 using concentrated NaOH.

TLC solvent used for analysis of the intermediates and the final product was prepared from ethyl acetate and hexane in a ratio of 1:2.

Fe-solution for the iron challenge was prepared by measuring 0.14 g of $Fe(III)NO_3$ and diluting it to 5 ml of purified water to obtain 27 mg/ml iron solution.

7.2. Methods

7.2.1. Synthesis of the precursor for radiolabeling

Synthesis of HBED-CC-tetrazines **3a** and **3b** are presented in figure 17.

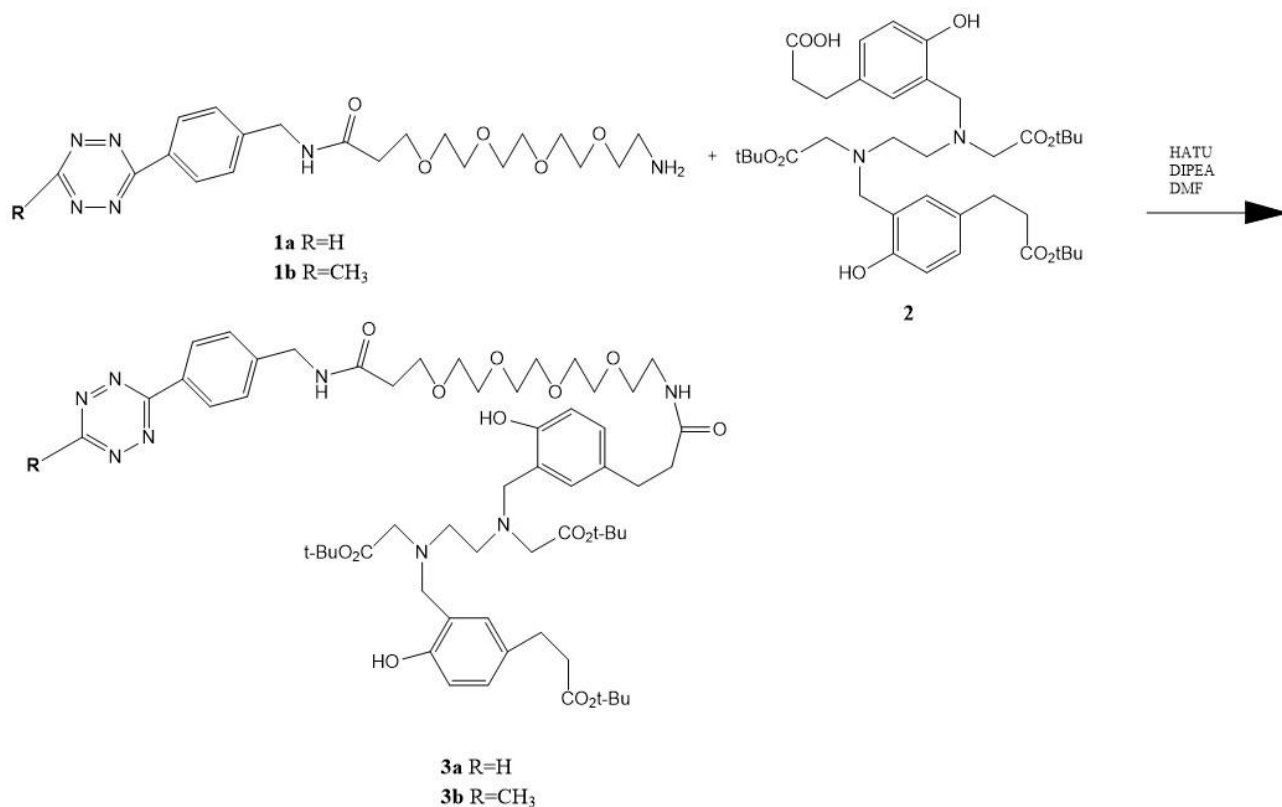


Figure 17. Synthesis of HBED-CC-tetrazines **3a** and **3b**.

Tert-butyl 3-(3-(((2-((5-(1-(4-(114,2,4,5-tetrazin-3-yl)phenyl)-3,19-dioxo-6,9,12,15-tetraoxa-2,18-diazahenicosan-21-yl)-2-hydroxybenzyl)(2-(tert-butoxy)-2-oxoethyl)amino)ethyl)(2-(tert-butoxy)-2-oxoethyl)amino)methyl)-4-hydroxyphenyl)propanoate (3a).

HBED-CC-tris(t-Bu)-ester **2** (50 mg, 0.071 mmol, 1.3 eq) was dissolved in 0.45 ml of DMF and added to a 100 ml flask. HATU (58 mg, 0.15 mmol, 2.8 eq) was added to the reaction flask with 0.35 ml DMF and the mixture was let to stir for 10 minutes in dark and under argon atmosphere. Tetrazine **1a** (25 mg, 0.053 mmol, 1 eq) was first dissolved in 0.6 ml DMF and then added to the reaction mixture carefully using a syringe and a needle. The reaction mixture was then let to stir for 20 minutes in dark and under argon atmosphere. Finally, DIPEA (33 μ l, 0.19 mmol, 3.5 eq) was added to the mixture and the reaction mixture

was let to stir for 48 hours in room temperature, covered from light and under argon atmosphere. The progress of the reaction was followed by TLC every 24 hours during the reaction. Ethyl acetate: hexane (1:2) solution was used in the silica TLC as a solvent. $R_f(\mathbf{3a}) = 0.46$.

Extractions were made to change and remove the solvent. First, 10 ml of ethyl acetate was added to the reaction mixture. Extractions were made six times using liquid-liquid extraction. First 5 ml of purified water was added to reaction mixture and the separation funnel was shaken gently. Pink product stayed in the upper level at the organic solvent. When two layers clearly separated, the lower aqueous layer was drained into a beaker. After that, the same procedure was repeated five times with 5 ml of 5% LiCl. After extractions, the organic layer was dried using $MgSO_4$, filtrated and evaporated to dryness using rotavapor. TLC was made to make sure the product stayed with the right layer during extractions. Ethyl acetate: hexane (1:2) solution was used in the silica TLC as a solvent. The final product was purified with high-performance liquid chromatography. HPLC device and parameters are presented in table 2. Yield: 44 mg (75 %) as a pink solid. Purity > 95%.

1H NMR (300 MHz, CD_3CD): δ 1.39-1.48 (27H, 1.39 (s), 1.39 (s), 1.39 (s)), δ 2.00 (2H, tt, $J = 5$ Hz), δ 2.44 (6H, t), δ 2.76-2.88 (8H, t), δ 3.02 (4H, t, $J = 3$ Hz), δ 3.20 (2H, t, $J = 7$ Hz), δ 3.42 (2H, t, $J = 5$ Hz), δ 3.60 (2H, s ; 2H, s), δ 3.61-3.77 (16H, 3.64 (t, $J = 4$ Hz), 3.64 (t, $J = 3$ Hz), 3.65 (t, $J = 4$ Hz), 3.64 (t, $J = 4$ Hz), 3.65 (t, $J = 3$ Hz), 3.64 (t, $J = 4$ Hz), 3.67 (s), 3.71 (t, $J = 6$ Hz)), δ 4.53 (2H, s), δ 6.69 (1H, dd, $J = 9, 1$ Hz), δ 6.89 (4H, dd), δ 7.00 (1H, dd, $J = 2, 1$ Hz), δ 7.56 (2H, ddd, $J = 8.0, 2.2, 0.4$ Hz), δ 7.98 (2H, ddd, $J = 8, 2, 1$ Hz), δ 8.49 (1H, s).

ESI-MS[M+H]⁺ m/z calculated 1117.6107 for $C_{58}H_{84}N_8O_{14}^+$, found 1117.6332.

Table 2. HPLC device and parameters for the purification of products **3a** and **3b**.

| Parameter | | Value |
|--|------------------|-------------------------|
| High-performance chromatography | liquid | Shimadzu |
| Column | | Waters symmetryPrep C18 |
| - Length | | 300 mm |
| - Inner diameter | | 7,8 mm |
| - Particle size | | 7 μm |
| Injection method | | Manual injection |
| Detector | | UV/VIS-detector |
| Solvents | | ACN/water |
| Method | Time(min) | ACN% |
| - Gradient | 1 | 5 |
| | 2 | 50 |
| | 4 | 90 |
| | 12 | 100 |
| | 13 | 100 |
| | 15 | 5 |

Tert-butyl 3-(3-(((2-(tert-butoxy)-2-oxoethyl)(2-((2-(tert-butoxy)-2-oxoethyl)(2-hydroxy-5-(1-(4-(1-methyl-1H,2,4,5-tetrazin-3-yl)phenyl)-3,19-dioxo-6,9,12,15-tetraoxa-2,18-diazahenicosan-21-yl)benzyl)amino)ethyl)amino)methyl)-4-hydroxyphenyl)propanoate (3b).

HBED-CC-tris(t-Bu)-ester **2** (59 mg, 0.084 mmol, 1.5 eq) was dissolved in 0.5 ml of DMF and added to a 100 ml flask. HATU (60 mg, 0.16 mmol, 2.8 eq) was added to the reaction flask with 0.3 ml DMF and the mixture was let to stir for 10 minutes in dark and under argon atmosphere. Tetrazine **1b** (25 mg, 0.056 mmol, 1 eq) was first dissolved in 1 ml DMF and then added to the reaction mixture carefully using a syringe and a needle. The reaction mixture was then let to stir for 20 minutes in dark and under argon atmosphere. Finally, DIPEA (34 μl, 0.20 mmol, 3.5 eq) was added to the mixture and the reaction mixture was let to stir for 48 hours in room temperature, covered from light and under argon atmosphere.

The progress of the reaction was followed by TLC every 24 hours during the reaction. Ethyl acetate: hexane (1:2) solution was used in the silica TLC as a solvent. $R_f(\mathbf{3b}) = 0.38$

After that, 10 ml of ethyl acetate was added to the reaction mixture. Extractions were made six times using liquid-liquid extraction. First 5 ml of purified water was added to reaction mixture and the separation funnel was shaken gently. Pink product stayed in the upper level at the organic solvent. When two layers clearly separated, the lower aqueous layer was drained into a beaker. After that, the same procedure was repeated five times with 5 ml of 5% NaCl. After extractions, the organic layer was dried using $MgSO_4$, filtrated and evaporated to dryness using rotavapor. TLC was made to make sure the product stayed with the right layer during extractions. Ethyl acetate: hexane (1:2) solution was used in the silica TLC as a solvent. The final product was purified with high-performance liquid chromatography. HPLC device and parameters are presented in table 2. Yield: 47 mg (76 %) as a pink solid. Purity > 95%.

1H -NMR (300 MHz, CD_3CD): δ 1.35 (27H, s), δ 2.55 (9H, t), δ 2.83-2.90 (4H, 2.75 (t, $J = 4.4$ Hz), 2.79 (t, $J = 4.4$ Hz), (4H, 2.86 (t, $J = 6.8$ Hz), 2.86 (t, $J = 7.4$ Hz)), δ 3.08 (4H, t, $J = 2.7$ Hz), δ 3.17 (2H, t, $J = 6.8$ Hz), δ 3.30 (2H, t, $J = 4.8$ Hz), 3.57-3.74 (3.57 (2H, s), 3.59 (2H, s), 3.64(16H, t, $J = 4.2$ Hz), δ 4.53 (2H, s), δ 7.57 ((2H, ddd, $J = 7.8, 1.5, 0.4$ Hz), (1H, dd, $J = 8.5, 0.4$ Hz), (4H, 6.85 (dd, $J = 8.5, 2.4$ Hz), (dd, $J = 8.5, 2.4$ Hz), (dd, $J = 8.5, 0.4$ Hz), (dd, $J = 2.4, 0.4$ Hz)), (1H, dd, $J = 2.4, 0.4$ Hz), δ 8.51 (2H, ddd, $J = 7.8, 1.6, 0.4$ Hz), δ 10.34 (H, -OH).

ESI-MS[M+H]⁺ m/z calculated 1131.6342 for $C_{59}H_{87}N_8O_{14}^+$, found 1131.6661.

7.2.1.1. Deprotection reaction

Deprotection reaction of HBED-CC-tetrazine to form deprotected compound **4b** is presented in figure 18.

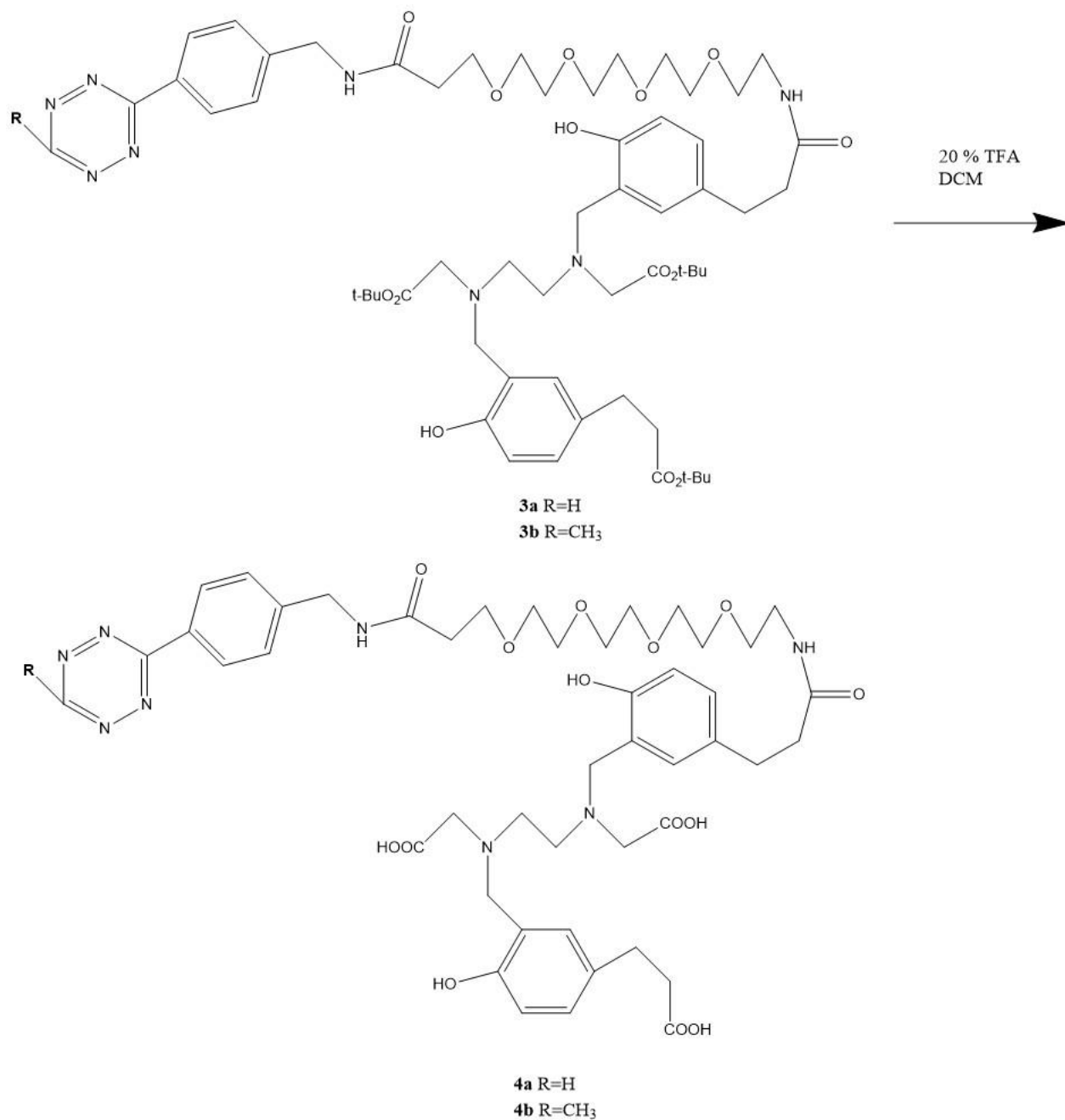


Figure 18. The deprotection reaction of **3b** to form deprotected compound **4b**.

3-(3-(((carboxymethyl)(2-((carboxymethyl)(2-hydroxy-5-(1-(4-(1-methyl-1H,2,4,5-tetrazin-3-yl)phenyl)-3,19-dioxo-6,9,12,15-tetraoxa-2,18-diazahenicosan-21-yl)benzyl)amino)ethyl)amino)methyl)-4-hydroxyphenyl)propanoic acid (4b).

Purified product **4b** (3 mg, 0.0027 mmol) was weighted and added to a flask. DCM (4 ml) and TFA (1 ml, 0.013 mmol) were combined in a small flask and then added to the reaction mixture. After addition, reaction was let to stir in room temperature for 24 hours. Para film and folio were used around the flask to avoid evaporation and light exposure.

After 24 hours, reaction was stopped and TLC was made to make sure the reaction was completed. TLC silica plate was first let to run in 1:1 ethyl acetate: hexane solvent and then dipped in ethanol solution of bromocresol green. $R_f(\mathbf{4b}) = 0.72$. Yield(**4b**) = 1.5 mg (60 %) as a pink oil. Purity > 99 %.

$^1\text{H NMR}$ (300 MHz, CD_3CD): δ 1.96 (2H, tt, $J = 7, 5$ Hz), δ 2.43 (9H, t), δ 2.74 (6H, t), δ 2.97 ((4H, t, $J=5$ Hz)), (4H, t, $J = 7$ Hz), (4H,t, $J = 3$ Hz)), δ 3.44 (2H, t, $J = 4.8$ Hz), δ 3.96 (16H, t), δ 6.98 (1H, dd, $J = 8.5, 2.4$ Hz). The tetrazine peaks are not visible in the spectrum.

ESI-MS[M+H]⁺ m/z calculated 963.4464 for $\text{C}_{47}\text{H}_{63}\text{N}_8\text{O}_{14}$, found 963.4198.

7.2.2. Radiosynthesis of ^{68}Ga

Deprotected product **4b** was labeled with ^{68}Ga (figure 19).

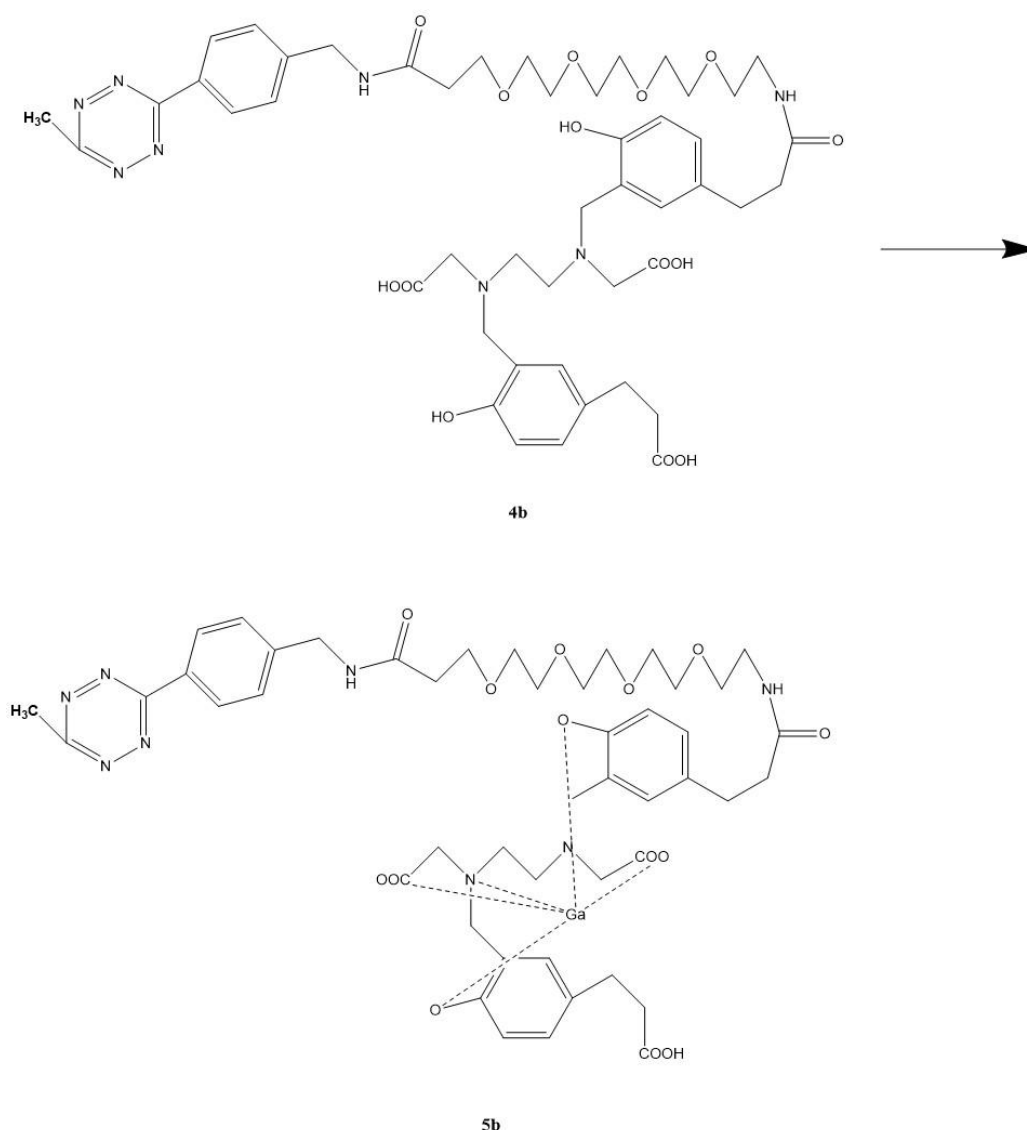


Figure 19. Radiosynthesis of deprotected product **4b**.

Radiosynthesis of [^{68}Ga]-3-(3-(((carboxymethyl)(2-((carboxymethyl)(2-hydroxy-5-(1-(4-(1-methyl-1H-tetrazin-3-yl)phenyl)-3,19-dioxo-6,9,12,15-tetraoxa-2,18-diazahenicosan-21-yl)benzyl)amino)ethyl)amino)methyl)-4-hydroxyphenyl)propanoic acid (**5b**).

The $^{68}\text{Ge}/^{68}\text{Ga}$ - generator was first eluted with 0, 1 M ultrapure HCl-solution to achieve ^{68}Ga -solution as $^{68}\text{Ga}^{3+}$ - ion. Elution volume was 10 ml and an average activity in that

amount was 200 MBq. After the addition of ^{68}Ga solution (300 μl , 6 MBq, at SOS) to vial containing **4b** (0.5 mg) dissolved in 200 μl of 1.5 M HEPES (pH=7.5), the pH of the labelling solution was adjusted to 4 with 1 M HCl (about 40 μl). When the pH was adjusted, and checked with pH paper, the samples were left to incubate in 85° for 20 minutes. After incubation, the radiolabelling yield was determined using radio-HPLC and TLC. The solvent used for TLC was 10 mM PBS with pH=7.4. The TLC was then analysed with TLC scanner. For the radio-HPLC, water and MeOH solvents were used. Conditions for HPLC are presented in table 3. **5b**: Radiochemical yield (DCY): 96 %, radiochemical purity: >98 % (TLC), 96 % (HPLC).

Table 3. HPLC parameters for determining radiolabeling yield from the reaction mixture and radiochemical purity of the product **5b**.

| Parameter | | Value |
|--|---------------|---------------------------------|
| High-performance chromatography | liquid | Shimadzu |
| Column | | Agilent pursuit XRs C18 |
| - Length | | 250 mm |
| - Inner diameter | | 4,6 mm |
| - Particle size | | 5 μm |
| Injection method | | Manual injection |
| Detector | | UV/VIS-detector, Radio-detector |
| Solvents | | MeOH/water |
| Method | | Time(min) MeOH% |
| - Gradient | | 1 1 |
| | | 3 25 |
| | | 6 50 |
| | | 12 100 |
| | | 15 1 |

7.2.3. Determining the lipophilicity

The lipophilicity of the compound **5b** was determined using a shake flask method. The distribution coefficient of the product was measured between 1-octanol and 20 mM phosphate buffer in pH = 7.4. First, same amount (5 ml) of both solvents were added to centrifuge tube. Then 200 μ l of the radiolabelled product was added and the activity of the content was measured using a carpenter dosimeter. The tube was then shaken vigorously for 1-2 minutes before moving the content of the tube to extraction funnel. The phases were then let to separate for 10 minutes. The activities of the organic and aqueous phase were then determined with the carpenter dosimeter as well as with a gamma counter. The logP value can be calculated from equation

$$\log P = \log \frac{\text{Solute}_{\text{octanol}}}{\text{Solute}_{\text{water}}}$$

(1)

The P value (partition coefficient) is a ratio between compounds concentration in octanol divided by compounds concentration in water. However, with radioactive substances, radioactivity concentration is used as a parameter instead of concentration.

7.2.4. The Fe challenge experiment and the stability of the product **5b**

For Fe-challenge, two samples were prepared. First sample was used as a control containing 200 μ l 1.5 M HEPES buffer (pH 7.5), 100 μ l of the radiolabelled product **5b** and 100 μ l 0.1 M HCl. The other sample contained 200 μ l 1.5 M HEPES (pH 7.5), 100 μ l of the radiolabelled product **5b** and 100 μ l of FeNO₃-solution (27 mg/ml of Fe (III)). The samples were stored in +37° and measured during different intervals with a radio-HPLC as well as with a radio-TLC (Whattman paper). The times intervals used were 0h, 1h, 2h, 3h, 4h and 6h. For TLC, 100% MeOH was used as a solvent.

8. Results and discussion

8.1. Optimizing the synthesis of the precursor for radiolabeling

The synthesis of the HBED-CC-tetrazine-PEG4 was made from two starting reagents, HBED-CC chelating reagent and tetrazine-PEG4-amine (**1a** and **1b**) (figure 20). Reaction conditions, choice of the coupling reagent and method of purification were all tested to get the optimum yield from the precursor synthesis. Two different tetrazines (**1a** and **1b**) were used in the synthesis. Molecular masses of the obtained products were 1117 g/mol for **3a** and 1131 g/mol for **3b**. Coupling reaction between HBED-CC and tetrazine-PEG4-amine (**1a**) was attempted with three different coupling reagents, TSTU, HATU and EDC. When best coupling reagent was chosen, also methyltetrazine-PEG4-amine (**1b**) was used as a starting material.

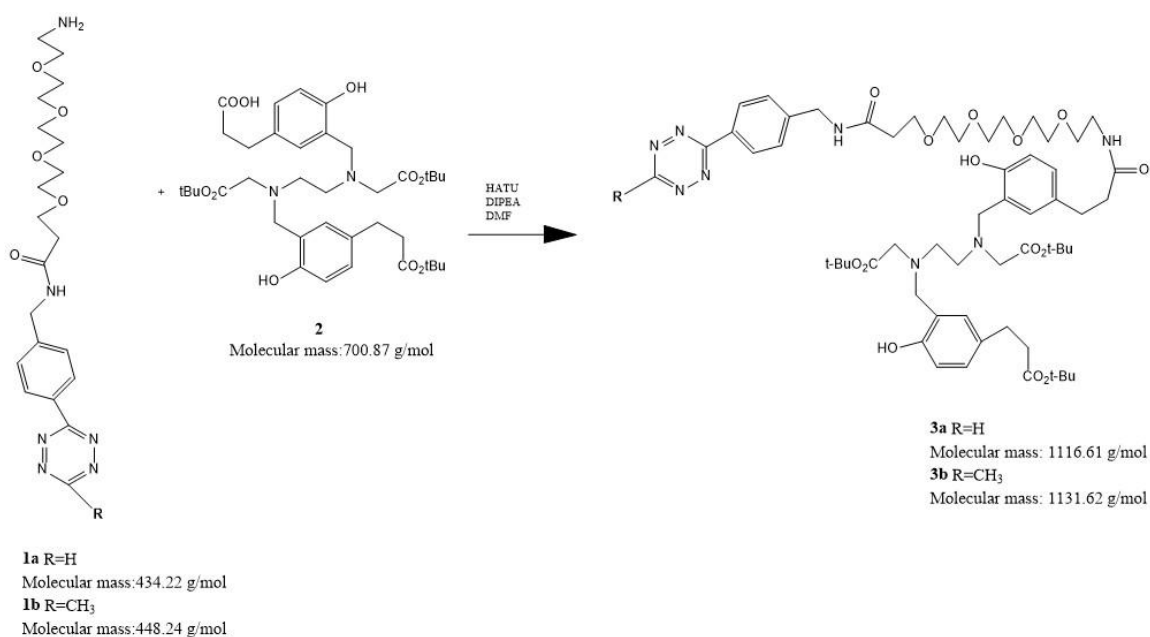


Figure 20. Coupling reaction of HBED-CC and tetrazine-PEG4-amine (**1a** and **1b**).

Coupling reaction between HBED-CC and tetrazine-PEG4-amine was first attempted with coupling reagent TSTU. Reaction time varied from 12 hours to 24 hours. However, with that

reaction, the desired product was not obtained. This was stated when a sample taken after extractions was measured by a mass spectrometry (figure 21).

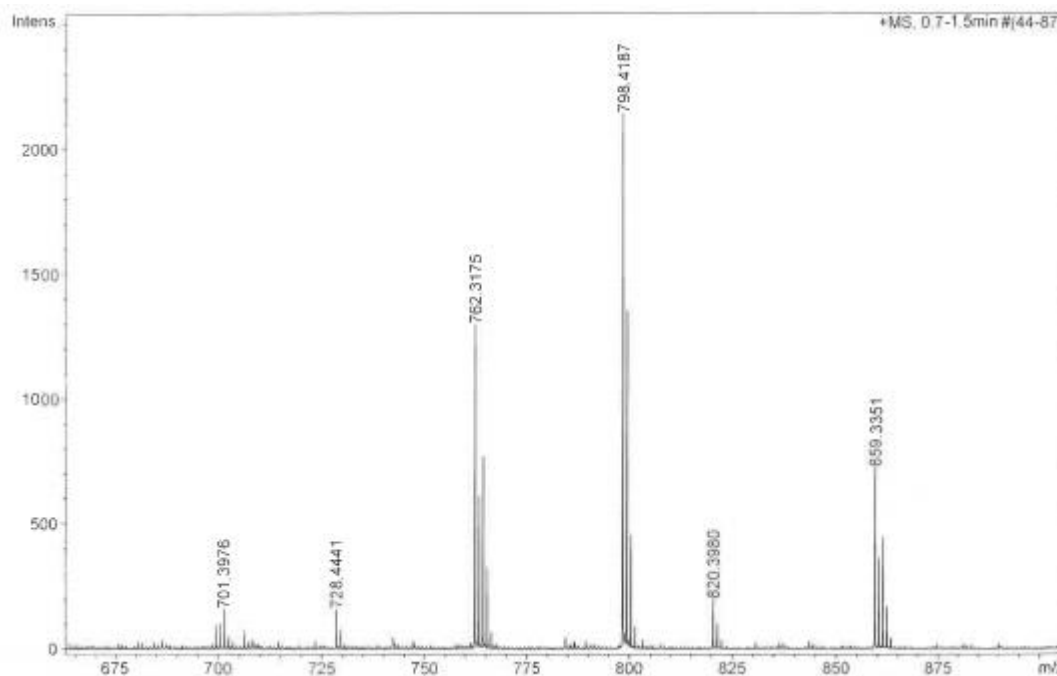


Figure 21. MS spectrum of the coupling reaction using coupling reagent TSTU. The desired product **3a** (1117 g/mol) cannot be seen in the spectrum.

From the MS spectrum can be seen that product with a molecular mass of 1117 g/mol cannot be seen. In contrast, multiple smaller peaks appear among the HBED-CC starting material (MW= 700 g/mol) which refers that the desired reaction did not occur.

After unsuccessful reaction with TSTU, another coupling reagent, HATU, was tested. Reaction succeeded with a yield of 60 % after 24 hours' reaction time. Reaction time was prolonged to 48 hours which lead to better yield of 72 %. However, another coupling reagent was still tried to get better yield with a shorter reaction time.

Next reaction was attempted with EDC. Reaction time was 48 hours which resulted to a yield of 72 % before purification. However, in this reaction the obtained product turned from pink to brown during the following night. Product was injected to HPLC where multiple peaks were seen which indicated that the product had decomposed. This might have been due to wrong storage conditions (in room temperature) or the EDC might have been from an old

batch. However, as HATU had given relatively good results, no further experiments were done using EDC.

Based on these results, reaction was to be continued using HATU as a coupling reagent. Coupling reaction was repeated several times using different conditions with reaction yields varying from 65 % to 85 %. Reaction time varied from 8 hours to 96 hours, but the maximum yield was achieved with 48-hour reaction time in room temperature. Reaction was also performed in higher temperature, in 85 °C. Reaction yield turned out to be quite good, almost 75 %. However, it was chosen not to use higher temperature in future experiments because the reaction was easier to perform in room temperature and the yield didn't differ that much. Still, it was significant to see that reaction in 85 °C could also work, because radiolabeling with ⁶⁸Ga occurs in that temperature. Reaction was finally optimized to 48 hours in room temperature which resulted to yield of 82 ± 4 %.

The obtained product was purified using two different methods. Silica column chromatography and High Performance Liquid Chromatogram (HPLC) were both used and compared to achieve the best recovery of the product. From these two methods, HPLC was chosen as a better purification technique. HPLC was faster, easier and it led to a better recovery of the product.

However, silica column chromatography was also tested. Before purification, the product was first dissolved in 6 ml of ethyl acetate. After that, the reaction mixture was divided into two parts so the purification could be done in smaller batches to maximize the yield. One batch contained approximately 10 mg of the product. Both items solvents were then evaporated with rotavapor for the purification. Purification was made using silica which is a polar absorbent. That means that the more polar compounds tend to stay with the stationary phase while the nonpolar compounds travel through the column faster. Before starting the purification, the column was first prepared with 10 ml of ethyl acetate.

When the column had been prepared accordingly, the elution of the product could be started. First 10 ml of hexane was added to the column carefully using funnel so the surface of the silica didn't get disturbed while the liquid was being poured. The flow rate of the solvent was adjusted using air pump. Five 2 ml fractions were collected into small tubes. When the solvent level was almost at the surface of the silica, 10 ml of 1:1 ethyl acetate: hexane-solution was added. After five 2 ml fractions were collected, 10 ml of ethyl acetate was added to the column and fractions were again collected. Finally, the column was washed

with 10 ml of EtOH to make sure that every compound had passed through the silica column. To verify the right fraction with the product, TLC was made with a small drop from every test tube. A small drop from pure sample of the product was also placed to the TLC plate alongside other drops. The TLC plate was then sprayed with ninhydrin, heated and the appeared marks were compared with the mark of the standard to recognise the right fractions. Silica column purification turned out to be very slow and not that effective of a method. For that reason, HPLC was chosen as a purification method. Even though, also the HPLC purification took quite a long time due to columns ability to handle only small batches. Also, the product had to be purified two times to get pure product. Reason for second purification was the residue of the starting material, HBED-CC shown in the mass spectrometry spectrum. The HPLC picture of pure product (**3b**) is shown in a figure 22. Retention time was observed to be 8.6 minutes for **3b** and 8.5 minutes for **3a**.

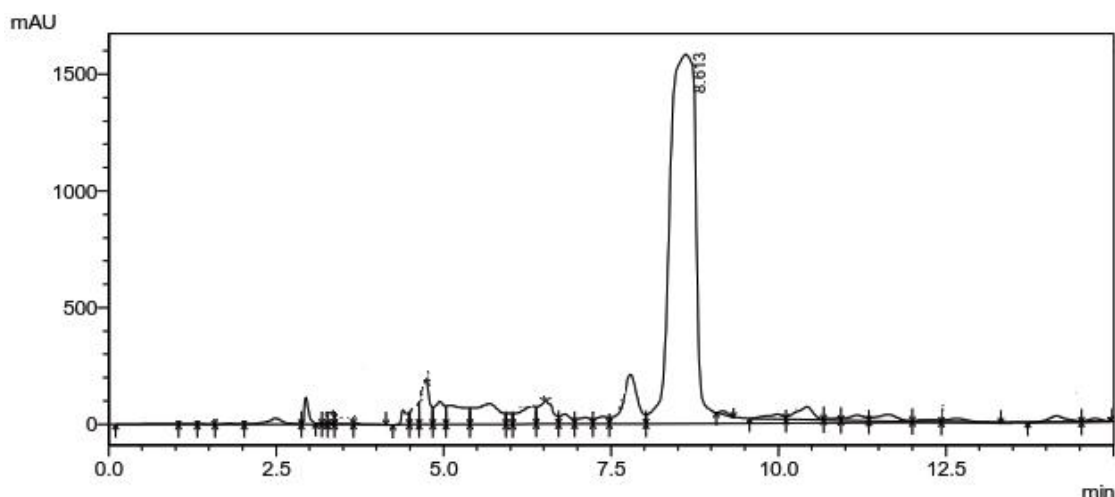


Figure 22. Purified product (**3b**) injected to HPLC. Retention time of the product was 8, 7 minutes. Retention time for **3a** did not differ significantly (8.5 minutes). UV/VIS detector was used with a wavenumber of 254 nm. Retention time of HBED-CC was 7,5 minutes and tetrazine was 2,9 minutes.

Purified products **3a** and **3b** were characterized with MS and NMR. Pictures of MS-spectrum and ^1H NMR spectrum are in the appendix 1 and 2 for **3a** and in appendix 3 and 4 for **3b**.

Deprotection reaction was made after the product (**3b**) was discovered to be purified. Deprotection reaction was made to remove the protecting tert-butyl-groups so the radiolabeling with ^{68}Ga would be possible and the coordination complex could be formed.

In the deprotection reaction, only TFA was used as an acid for the deprotection of tert-butyl-groups. The reaction time, however, was altered couple of times. Deprotection of the starting material, HBED-CC, was used in the optimizing of the reaction time. Reaction time was first only 4 hours, but the reaction didn't complete during this time. Reaction time was then increased to 12 hours and finally to 24 hours, which was demonstrated to be optimal reaction time. Reactions progress was monitored with a TLC using bromocresol as a dying agent. Bromocresol can be used to reveal compounds with functional groups whose pK_a is below 5. Deprotected carboxylic groups appear on the silica plate as yellow spots on a green background.

Deprotected product was characterized with MS and NMR. Pictures of MS and ^1H NMR spectrums are in the appendix 5 and 6 for **4b**. However, the ^1H NMR characterization of the obtained deprotected product **4b** was not successful. ^1H NMR spectrum does not show peaks around 6-9 ppm where the chemical shifts of tetrazines benzene rings hydrogens should be (figure 23).

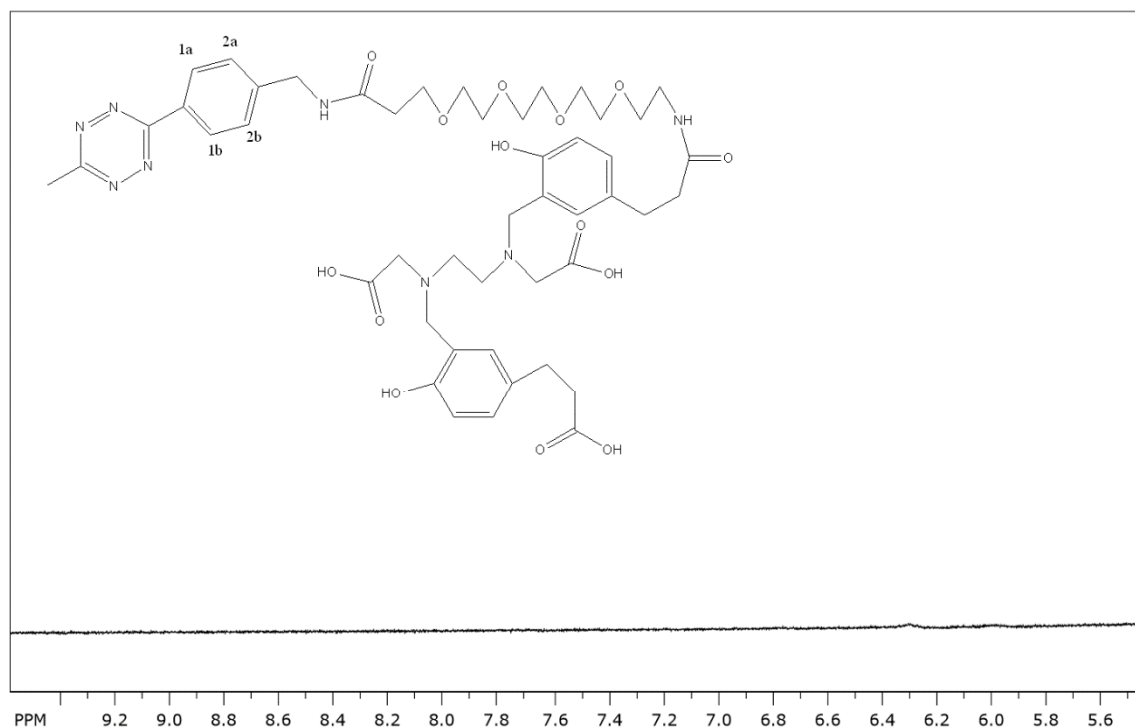


Figure 23. Zoom up of the ^1H NMR spectrum of deprotected product **4b** around 6-9 ppm where the peaks for tetrazines benzene rings hydrogens 1a, 1b and 2a, 2b should be seen.

This might indicate that the bond between tetrazine and HBED-CC was broken down in the deprotection reaction with TFA although this is not likely due to the extremely strong amide bond between them. Decomposition of the molecule from some other part might still be possible. Still, MS spectrum shows the right mass of 963 g/mol for the product **4b** (appendix 5). Reason for bad quality of NMR spectrum could be the too small amount of sample for such a large molecule. For the same reason, ^{13}C NMR spectra could not be measured. However, without proper characterization data, the right structure of the molecule cannot be guaranteed.

8.2. Radiolabeling with ^{68}Ga

Radiolabeling with ^{68}Ga was first tested with deprotected HBED-CC. In this experiment, two different temperatures were used and the incubation time was also altered. Samples were incubated in room temperature and in 85 °C, and the incubation time was altered from 5 minutes to 20 minutes. The best yield was gained with an incubation time of 20 minutes. Expectedly, the radiolabeling yield turned out to be very high, 97.9 % with the sample incubated in 85 °C and 95.8% for the sample in room temperature. HBED-CC labeled with ^{68}Ga was then injected to radio-HPLC and the retention time turned out to be 6.4 minutes. These conditions were then used in the radiolabeling process of the actual product **4b**.

For the product **4b**, the radiolabeling procedure was repeated several times using different amounts of the product. Amounts of precursor, obtained radiochemical yield and calculated specific activity are presented in table 4.

Table 4. The amount of precursor **4b** used in the radiolabeling and product yield and specific activity. Specific activity is calculated by dividing the starting activity by substance amount (Bq/mol).

| Precursor amount(nmol) | Product yield (%) | Specific activity (MBq/nmol) |
|------------------------|-------------------|------------------------------|
| 0,19 | 70 | 26,3 |
| 1,19 | 96 | 5,9 |
| 1,6 | 96 | 0,29 |

The starting activity varied from 5-5,8 MBq. To ensure the radiochemical purity, TLC was made from the product **5b** alongside free $^{68}\text{GaCl}_3$ from generator and the TLC paper was

scanned with autoradiography. [^{68}Ga] Ga-HBED-CC-tetrazine (**5b**) got carried from the starting line with eluent and no free $^{68}\text{GaCl}_3$ was left in the application level. Thus, the radiochemical purity for [^{68}Ga]Ga-HBED-CC-tetrazine (**5b**) got defined with a value of 98.2 % (figure 24).

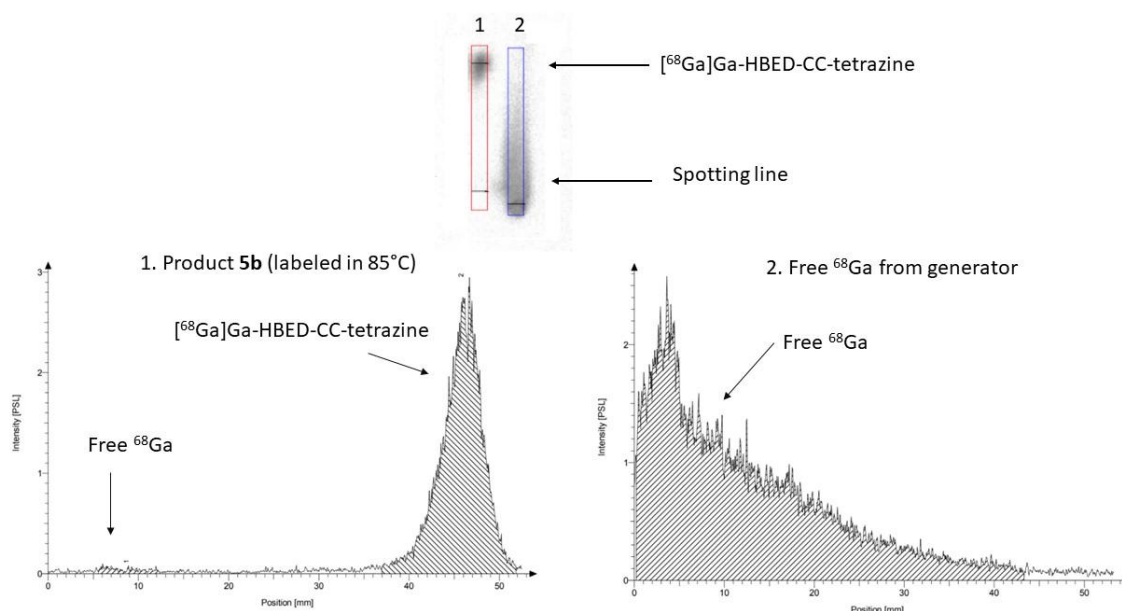


Figure 24. TLC made from spots of [^{68}Ga] Ga-HBED-CC-tetrazine (**5b**) and free $^{68}\text{GaCl}_3$ from generator. The eluent used for TLC was 10 mM PBS with pH=7.4. Obtained product **5b** can be seen in area of 40-50 mm as a big peak in spectrum 1.

After incubation time, complex formation was done and obtained labeled product **5b** was injected to radio-HPLC (figure 25).

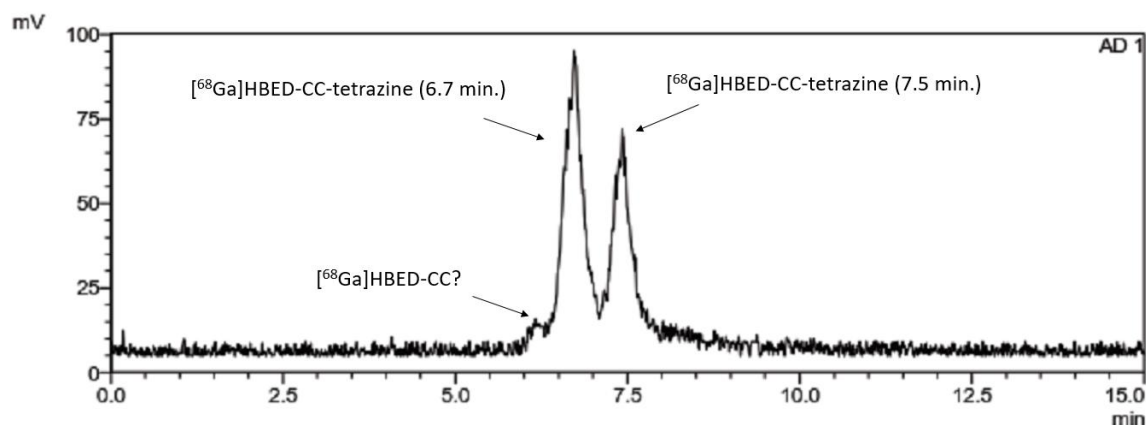


Figure 25. Radio-HPLC chromatogram of labeled product **5b**. 50 μl , 0,4 MBq was injected. Two peaks appear with retention times 6.7 and 7.5 minutes. A possible peak for labeled starting material HBED-CC can be seen with a retention time on 6.4 minutes.

Two peaks with retention time of 6.7 and 7.5 minutes appear. Retention time of labeled HBED-CC was 6.4 minutes and a small peak with that retention time can be seen in this spectrum also. This means that there might have been a small residue of unreacted HBED-CC in the sample. However, the amount of that residue seems to be insignificant.

To make sure product was completely labeled, $^{68}\text{GaCl}_3$ ($V= 10 \mu\text{l}$, $A= 0.2 \text{ MBq}$) straight from generator was injected to HPLC to determinate its retention time. As expected, hydrophilic $^{68}\text{GaCl}_3$ eluted from HPLC rapidly with a retention time of 2.6 minutes. Chromatogram of radio-HPLC of $^{68}\text{GaCl}_3$ is presented in figure 26.

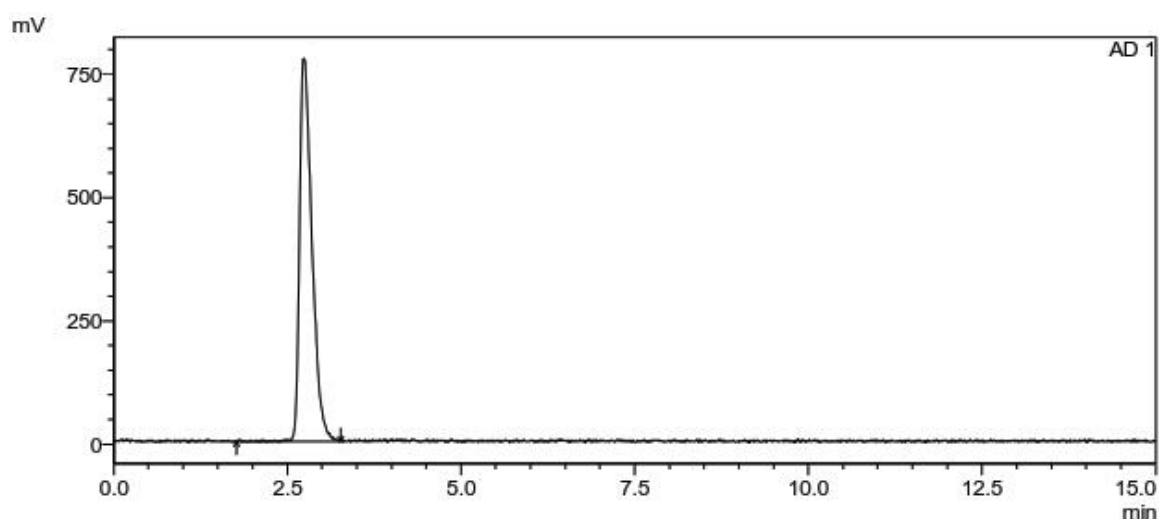


Figure 26. Radio-HPLC chromatogram of $^{68}\text{GaCl}_3$ injected to HPLC. Free $^{68}\text{GaCl}_3$ retention time is 2.7 minutes.

Two peaks appearing in the spectrum (figure 25) could be isomers caused of HBED-CC structures complex formation with ^{68}Ga . Possible isomers are presented in figure 27.

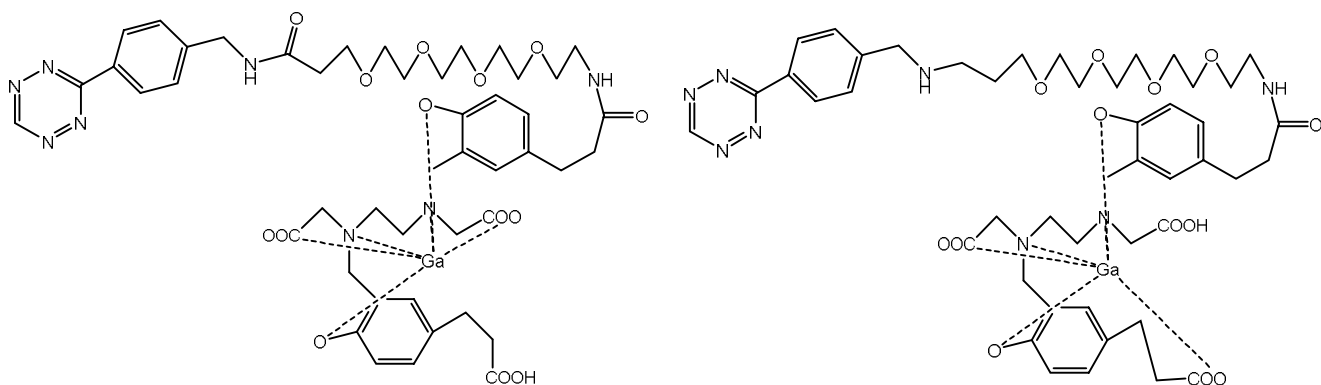


Figure 27. Possible isomers of the radiolabeled product **5b**.

As can be seen from the picture, ^{68}Ga can form coordination complex with the product either from one of the carboxylic acids or from amine group. Isomers of HBED-CC were investigated in a study by Eder et al. (2014). Isomer formation did not seem to affect radiolabeling procedure. However, it was stated that exact chemical nature of these complexes needed to be investigated more thoroughly to clarify more of their biological properties. Thus, when it comes to injecting this possible radiotracer to human body, isomer formation might affect the binding properties.

8.3. Determining the lipophilicity

The lipophilicity experiment was first tested with free ^{68}Ga in 0.1 M HCl solution. As expected, $^{68}\text{GaCl}_3$ turned out to be hydrophilic with a value of -1.59. The lipophilicity of the product was determined three times to achieve the average and standard deviation of the results. The results from each experiment are combined in a table 5.

Table 5. Results from lipophilicity test of **5b**.

| Experiment | A(organic) | A(aqueous) | logP |
|------------|------------|------------|-------|
| 1 | 0.068 | 0.832 | -1.08 |
| 2 | 0.039 | 0.745 | -1.28 |
| 3 | 0.042 | 1.25 | -1.47 |

Average logP value of the product **5b** turned out to be below zero with a value of -1.28 ± 0.19 . This means that the product is hydrophilic. For pretargeting purposes, low lipophilicity is

usually admirable for tetrazine to achieve maximum specific binding in *in vivo* conditions. During the experiment, lipophilicity of ^{68}Ga -DOTA-tetrazine complex was also determined. LogP value turned out to be even smaller with a value of -1.45.

Lipophilicity can be defined as the affinity of a molecule to a lipophilic environment. Low logP value corresponds to low lipophilicity. Low lipophilicity is admirable for downplaying nonspecific binding and to prevent redundant radioactivity for intestinal and liver as it makes the positioning of radiation source more difficult. The determination of logP value is especially important for a radiotracer, because lipophilicity rate affects greatly absorption, distribution, metabolism and excretion (ADME) of the compound in human body. Usually, very hydrophilic compounds are soluble in water and they have functional groups that can form ions. This leads the compound to clear rapidly through kidneys and to be unable to cross the blood-brain-barrier (Jolliet-Riant et al., 1999). For that reason, lipophilicity determinations are especially important in brain studies.

8.4. The Fe challenge experiment and the stability of the product **5b**

The iron challenge experiment as well as the stability test were performed in parallel during the same day. The radiolabelled product was challenged with Fe, to estimate the stability of the product in solution with excess Fe. The Fe solution was about 10 times more molar than the product **5b** molarity corresponding to the molarity of iron circulating in human body

Experiments for the iron challenge and the stability of the product were performed at the same time. For the first 3 hours' compound remained quite stable. Labeling percentages for product with and without iron from hours 3 to 6 are presented in the table 6.

Table 6. Labeling percentages after 3-6 hours with and without iron.

| Hours from labeling | Without Fe | With Fe |
|---------------------|------------|---------|
| 3 | 80 % | 44 % |
| 4 | 75 % | 45 % |
| 6 | 69 % | 48 % |

During this experiment, labeling with ^{68}Ga did give a labeling percentage of only 83 %. This might explain why compound seem to become so unstable after 3 hours. However,

iron seems to have some effect on ^{68}Ga -product complex. This is something that should be investigated in the future for a radiotracer should be able to resist Fe exchange in the complex.

Eder et al. (2008) did a stability test for [^{68}Ga]HBED-CC-mAb425 conjugate in human serum for 4 hours at 37 °C. The results showed that human serum did not affect the stability of the conjugate. Therefore, it is important to renew the stability test in human serum instead of using buffer.

The same research group did also a stability test for ^{68}Ga -labeled peptides using an excess of apo-transferrin (Eder et al. 2012). After 2 hours of incubation in 37 °C, ^{68}Ga was still associated with the peptide. This indicates that the HBED-CC complex should be able to withstand iron.

9. Conclusions and future work

Synthesis of HBED-CC-tetrazine-PEG4-amine was successfully optimized with suitable conditions. Reaction was done several times with reasonably high yield of 82 ± 4 %. However, the reaction time of the coupling reaction with HATU is relatively long and the shortening of this reaction time might be relevant in the future. There was some trouble with the purification of product. Purification process had to be done two, sometimes even three times to obtain pure product. This might have been because starting material HBED-CC had similar retention time than the product and therefore was hard to separate. Changing the HPLC method or column might have helped with the problem. Optimization of deprotection reaction was also successfully done with starting material HBED-CC. However, with the product **4b** characterization with NMR was not completely done which leaves the complete structure of compound unclear. Fortunately, MS spectrum gave the right mass, so we could move to the radiolabeling part with ^{68}Ga . However, NMR spectrums from the deprotected product **4b** need to be done in the future.

Radiolabeling of the product **4b** gave a good yield of 97 % and radiochemical purity turned out to be over 98 %. The possible isomer formation of HBED-CC is something to keep in mind to, as it has been reported also before. Luckily, two isomers didn't seem to affect the radiolabeling in any harmful way. However, as said before, if this kind of compound was to be injected to human patient, it should be investigated more thoroughly.

Iron challenge experiment and the stability test did not give promising results. However, like said before, radiolabeling occurred in the first place with a smaller radiochemical yield than what was usually obtained. There are several studies to achieve before product can be tested *in vivo*. The stability of product still needs some further investigations as the experiment in this master's thesis was done in buffer solution. Stability tests should be done in human serum instead of buffers to get more significant results. Iron challenge experiment however should be tested again with a better radiolabeling yield in the beginning. For the future, it is also better to do the challenge of the complex of nanoparticles/HBED-CC-tetrazine with free HBED-CC. Iron exchange in complex is crucial to determinate if radiotracer development is to be continued. In future, *in vivo* biodistribution studies are required to resolve compounds behaviour in human body and do determinate its suitability as PET imaging tracer.

Past several years have shown rapid development in the pretargeting approach and especially in the bioorthogonal chemistry mainly because of fast kinetics of click chemistry reactions and tetrazine bioorthogonal reactions. HBED-CC-tetrazine complex radiolabelled with ^{68}Ga brings an interesting and valuable addition to the area of PET imaging nuclear medicine.

10. References

- Abdelmoty I, Albericio F, Carpino LA, Foxman BM, Kates SA. Structural studies of reagents for peptide bond formation: Crystal and molecular structures of HBTU and HATU. *Lett Peptide Sci.* 1994;1(2):57-67.
- Aboagye EO, Price PM. Use of positron emission tomography in anticancer drug development. *Invest New Drugs.* 2003;21(2):169-181.
- Al-Warhi TI, Al-Hazimi HMA, El-Faham A. Recent development in peptide coupling reagents. *Journal of Saudi Chemical Society.* 2012;16(2):97-116.
- Bartholomä MD, Louie AS, Valliant JF, Zubieta J. Technetium and gallium derived radiopharmaceuticals: Comparing and contrasting the chemistry of two important radiometals for the molecular imaging era. *Chem Rev.* 2010;110.
- Blackman ML, Royzen M, Fox JM. Tetrazine ligation: Fast bioconjugation based on inverse-electron-demand Diels–Alder reactivity. *J Am Chem Soc.* 2008;130(41):13518-13519.
- Blom E, Velikyan I, Monazzam A, et al. Synthesis and characterization of scVEGF-PEG-[68Ga]NOTA and scVEGF-PEG-[68Ga]DOTA PET tracers. *J Labelled Compd Radiopharmaceut.* 2011;54(11):685-692.
- Boger DL. Diels-alder reactions of azadienes. *Tetrahedron.* 1983;39(18):2869-2939.
- Bolus NE, George R, Washington J, Newcomer BR. PET/MRI: The blended-modality choice of the future? *Journal of Nuclear Medicine Technology.* 2009;37(2):63-71.
- Bonardi M, Groppi F, Mainardi HS. High specific activity radioactive tracers: A powerful tool for studying very low level and long term exposure to different chemical forms of both essential and toxic elements. *Microchemical Journal.* 2002;73(1–2):153-166.
- Bos ES, Kuijpers WHA, Meesters-Winters M, et al. *In vitro* evaluation of DNA-DNA hybridization as a two-step approach in radioimmunotherapy of cancer. *Cancer Res.* 1994;54(13):3479.

Bottomley PA. NMR imaging techniques and applications: A review. *Rev Sci Instrum.* 1982;53(9):1319-1337.

Caraco' C, Aloj L, Eckelman WC. The gallium–deferoxamine complex: Stability with different deferoxamine concentrations and incubation conditions. *Applied Radiation and Isotopes.* 1998;49(12):1477-1479.

Chang C, Sharkey RM, Rossi EA, et al. Molecular advances in pretargeting radioimmunotherapy with bispecific antibodies 1 supported in part by USPHS grant R01-CA-84379 from the NIH and department of energy grant DE-FG01-00NE22941 (both to RMS). 1. *Molecular cancer therapeutics.* 2002;1(7):553-563.

De Hoffmann E, Stroobant V. *Mass spectrometry: Principles and applications.* Wiley; 2007.

Decristoforo C, Pickett RD, Verbruggen A. Feasibility and availability of ⁶⁸Ga-labelled peptides. *Eur J Nucl Med Mol Imaging.* 2012;39.

Del Guerra A. *Ionizing radiation detectors for medical imaging.* World Scientific; 2004.

Devaraj NK, Upadhyay R, Haun JB, Hilderbrand SA, Weissleder R. Fast and sensitive pretargeted labeling of cancer cells via tetrazine/trans-cyclooctene cycloaddition. *Angewandte Chemie (International ed.in English).* 2009;48(38):7013-7016.

Devaraj NK, Thurber GM, Keliher EJ, Marinelli B, Weissleder R. Reactive polymer enables efficient in vivo bioorthogonal chemistry. *Proc Natl Acad Sci U S A.* 2012;109(13):4762-4767.

Eder M, Wängler B, Knackmuss S, et al. Tetrafluorophenolate of HBED-CC: A versatile conjugation agent for ⁶⁸Ga-labeled small recombinant antibodies. *European Journal of Nuclear Medicine and Molecular Imaging.* 2008;35(10):1878-1886.

Eder M, Schäfer M, Bauder-Wüst U, et al. ⁶⁸Ga-complex lipophilicity and the targeting property of a urea-based PSMA inhibitor for PET imaging. *Bioconjugate Chem.* 2012;23(4):688-697.

- Eder M, Neels O, Miller M, et al. Novel preclinical and radiopharmaceutical aspects of [68Ga] ga-PSMA-HBED-CC: A new PET tracer for imaging of prostate cancer. *Pharmaceuticals*. 2014;7(7):779-796.
- Fani M, André JP, Maecke HR. 68Ga-PET: A powerful generator-based alternative to cyclotron-based PET radiopharmaceuticals. *Contrast Media Mol Imaging*. 2008;3.
- Fenn JB, Mann M, Meng CK, Wong SF, Whitehouse CM. Electrospray ionization for mass spectrometry of large biomolecules. *Science*. 1989;246(4926):64.
- Fowler JS, Ding Y, Volkow ND. Radiotracers for positron emission tomography imaging. *Seminars in Nuclear Medicine*. 2003;33(1):14-27.
- Gunther H. *NMR spectroscopy: Basic principles, concepts and applications in chemistry*. John Wiley & Sons; 2013.
- Green NM. Avidin. 1. the use of [14C] biotin for kinetic studies and for assay. *Biochem J*. 1963;89(3):585.
- Green, M. A., & Welch, M. J. Gallium radiopharmaceutical chemistry. *Nuclear Medicine and Biology*, 1989;16(5),435-448.
- Han S, Kim Y. Recent development of peptide coupling reagents in organic synthesis. *Tetrahedron*. 2004;60(11):2447-2467.
- He J, Liu G, Gupta S, Zhang Y, Rusckowski M, Hnatowich DJ. Amplification targeting: A modified pretargeting approach with potential for signal AmplificationProof of a concept. *Journal of Nuclear Medicine*. 2004;45(6):1087-1095.
- Heldt J, Kerzendörfer O, Mamat C, Starke F, Pietzsch H, Steinbach J. Synthesis of short and versatile heterobifunctional linkers for conjugation of bioactive molecules with (radio-) labels. *Synlett*. 2013;24(04):432-436.
- Heppeler A, Froidevaux S, Mäcke HR, et al. Radiometal-labelled macrocyclic chelator-derivatised somatostatin analogue with superb tumour-targeting properties and potential for receptor-mediated internal radiotherapy. *Chemistry – A European Journal*. 1999;5(7):1974-1981.
- Hnatowich DJ, Virzi F, Rusckowski M. Investigations of avidin and biotin for imaging applications. *J Nucl Med*. 1987;28(8):1294-1302.

- Ho CS, Lam C, Chan M, et al. Electrospray ionisation mass spectrometry: Principles and clinical applications. *The Clinical Biochemist Reviews*. 2003;24(1):3-12.
- Hou S, Choi J, Garcia MA, et al. Pretargeted positron emission tomography imaging that employs supramolecular nanoparticles with in vivo bioorthogonal chemistry. *ACS Nano*. 2016;10(1):1417-1424.
- Johnston RF, Pickett SC, Barker DL. Autoradiography using storage phosphor technology. *Electrophoresis*. 1990;11(5):355-360.
- Jolliet-Riant P, Tillement J. Drug transfer across the blood-brain barrier and improvement of brain delivery. *Fundam Clin Pharmacol*. 1999;13(1):16-26.
- Knight JC, Cornelissen B. Bioorthogonal chemistry: Implications for pretargeted nuclear (PET/SPECT) imaging and therapy. *Am.J.Nucl.Med.Mol.Imaging*. 2014;4(2):96-113.
- Kolb HC, Finn MG, Sharpless KB. Click chemistry: Diverse chemical function from a few good reactions. *Angewandte Chemie International Edition*. 2001;40(11):2004-2021.
- Lee SB, Kim HL, Jeong H, Lim ST, Sohn M, Kim DW. Mesoporous silica nanoparticle pretargeting for PET imaging based on a rapid bioorthogonal reaction in a living body. *Angewandte Chemie International Edition*. 2013;52(40):10549-10552.
- Lewellen TK. Recent developments in PET detector technology. *Phys Med Biol*. 2008;53(17):R317.
- Li G, Zhang H, Zhu C, Zhang J, Jiang X. Avidin-biotin system pretargeting radioimmunoimaging and radioimmunotherapy and its application in mouse model of human colon carcinoma. *World journal of gastroenterology*. 2005;11(40):6288.
- Li Z, Conti PS. Radiopharmaceutical chemistry for positron emission tomography. *Adv Drug Deliv Rev*. 2010;62(11):1031-1051.
- Maggi A, Ruivo E, Fissers J, et al. Development of a novel antibody-tetrazine conjugate for bioorthogonal pretargeting. *Organic & Biomolecular Chemistry*. 2016;14(31):7544-7551.
- Mathias CJ, Wang S, Lee RJ, Waters DJ, Low PS, Green MA. Tumor-selective radiopharmaceutical targeting via receptor-mediated endocytosis of gallium-67-deferoxamine-folate. *Journal of Nuclear Medicine*. 1996;37(6):1003-1008.

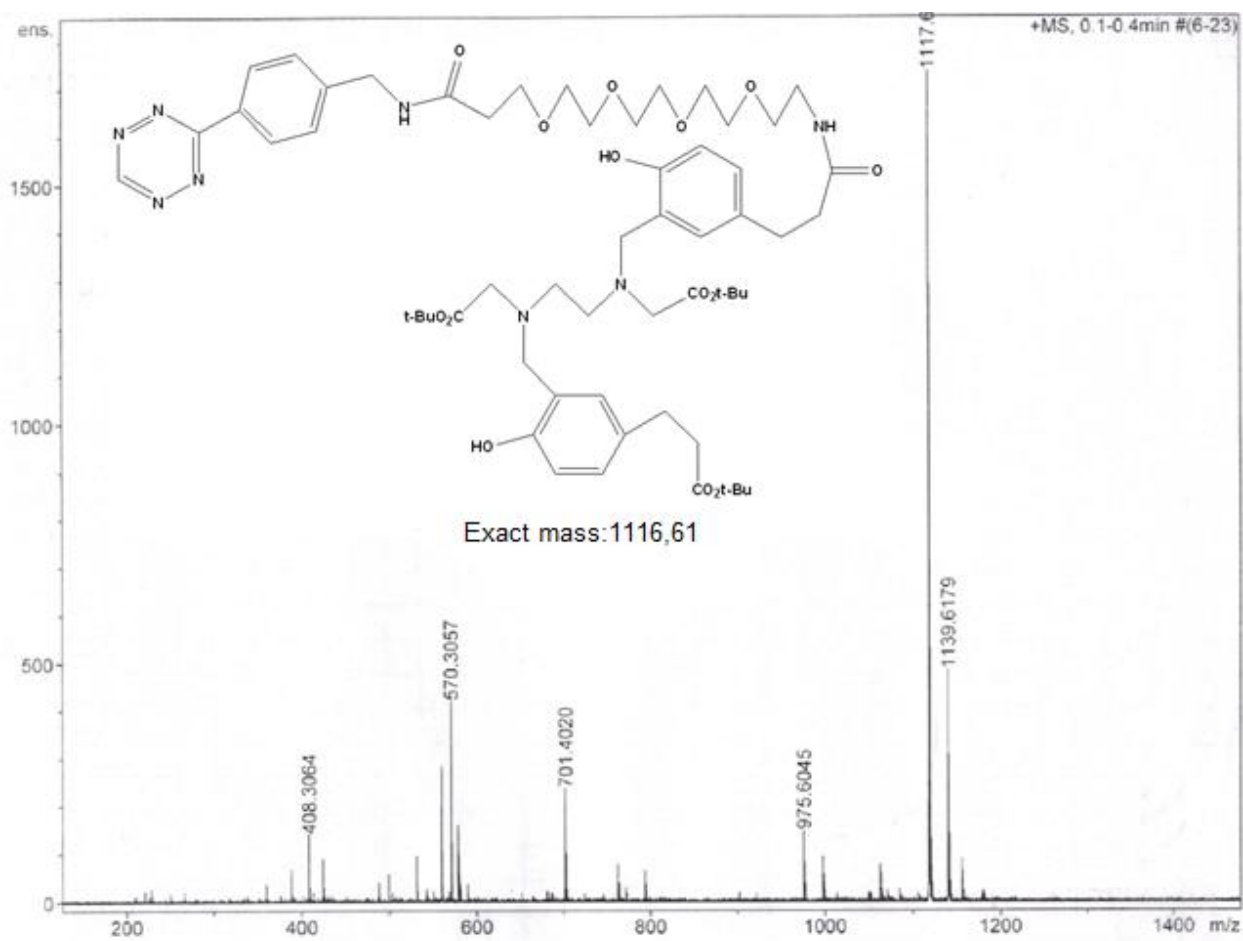
- Mokaleng BB, Ebenhan T, Ramesh S, et al. Synthesis, (68)Ga-radiolabeling, and preliminary in vivo assessment of a depsipeptide-derived compound as a potential PET/CT infection imaging agent. *BioMed Research International*. 2014;2015:284354.
- Montalbetti, Christian A G N, Falque V. Amide bond formation and peptide coupling. *Tetrahedron*. 2005;61(46):10827-10852.
- Nayak TK, Brechbiel MW. Radioimmunoimaging with longer-lived positron-emitting radionuclides: Potentials and challenges. *Bioconjug Chem*. 2009;20(5):825-841.
- Nichols B, Qin Z, Yang J, Vera DR, Devaraj NK. 68Ga chelating bioorthogonal tetrazine polymers for the multistep labeling of cancer biomarkers. *Chem Commun*. 2014;50(40):5215-5217.
- Notni J, Hermann P, Havlíčková J, et al. A triazacyclononane-based bifunctional phosphinate ligand for the preparation of multimeric 68Ga tracers for positron emission tomography. *Chemistry – A European Journal*. 2010;16(24):7174-7185.
- Notni J, Šimeček J, Hermann P, Wester HJ. TRAP, a powerful and versatile framework for gallium-68 radiopharmaceuticals. *Chem Eur J*. 2011;17.
- a Notni J, Plutnar J, Wester HJ. Bone seeking TRAP conjugates: Surprising observations and implications on development of gallium-68-labeled bisphosphonates. *EJNMMI Res*. 2012;2.
- b. Notni J, Pohle K, Wester H. Comparative gallium-68 labeling of TRAP-, NOTA-, and DOTA-peptides: Practical consequences for the future of gallium-68-PET. *EJNMMI Research*. 2012;2(1):28.
- Paganelli G, Riva P, Deleide G, Clivio A, Chiolerio F, Scassellati GA, Malcovati M, Siccardi AG. In vivo labelling of biotinylated monoclonal antibodies by radioactive avidin: a strategy to increase tumor radiolocalization. *Int J Cancer Suppl*. 1988;2:121–125.
- Pearson RG. Hard and soft acids and bases. *J Am Chem Soc*. 1963;85(22):3533-3539.
- Phelps ME, Hoffman EJ, Mullani NA, Ter-Pogossian MM. Application of annihilation coincidence detection to transaxial reconstruction tomography. *Journal of Nuclear Medicine*. 1975;16(3):210-224.

- Ray Banerjee S, Chen Z, Pullambhatla M, et al. Preclinical comparative study of ⁶⁸Ga-labeled DOTA, NOTA, and HBED-CC chelated radiotracers for targeting PSMA. *Bioconjugate Chem.* 2016;27(6):1447-1455.
- Reardan DT, Meares CF, Goodwin DA, et al. Antibodies against metal chelates. *Nature.* 1985;316(6025):265-268.
- Reiner T, Zeglis BM. The inverse electron demand Diels–Alder click reaction in radiochemistry. *J Labelled Compd Radiopharmaceut.* 2014;57(4):285-290.
- Rossin R, Renart Verkerk P, van den Bosch S, et al. In Vivo chemistry for pretargeted tumor imaging in live mice. *Angewandte Chemie International Edition.* 2010;49(19):3375-3378.
- Rossin R, van dB, ten Hoeve W, et al. Highly reactive trans-cyclooctene tags with improved stability for Diels–Alder chemistry in living systems. *Bioconjugate Chem.* 2013;24(7):1210-1217.
- Saxon E, Armstrong JI, Bertozzi CR. A “traceless” Staudinger ligation for the chemoselective synthesis of amide bonds. *Org Lett.* 2000;2(14):2141-2143.
- Schöder H, Erdi YE, Larson SM, Yeung HWD. PET/CT: A new imaging technology in nuclear medicine. *European Journal of Nuclear Medicine and Molecular Imaging.* 2003;30(10):1419-1437.
- Šimeček J, Schulz M, Notni J, et al. Complexation of metal ions with TRAP (1,4,7-triazacyclononane phosphinic acid) ligands and 1,4,7-triazacyclononane-1,4,7-triacetic acid: Phosphinate-containing ligands as unique chelators for trivalent gallium. *Inorg Chem.* 2012;51(1):577-590.
- Staudinger H, Meyer J. Über neue organische phosphorverbindungen III. phosphinmethylderivate und phosphinimine. *Helv Chim Acta.* 1919;2(1):635-646.
- Stickney DR, Anderson LD, Slater JB, et al. Bifunctional antibody: A binary radiopharmaceutical delivery system for imaging colorectal carcinoma. *Cancer Res.* 1991;51(24):6650-6655.
- Vallabhajosula, S. *Molecular Imaging; Radiopharmaceuticals for PET and SPECT*; Springer- Verlag Berlin Heidelberg. 2009; s.66-82.

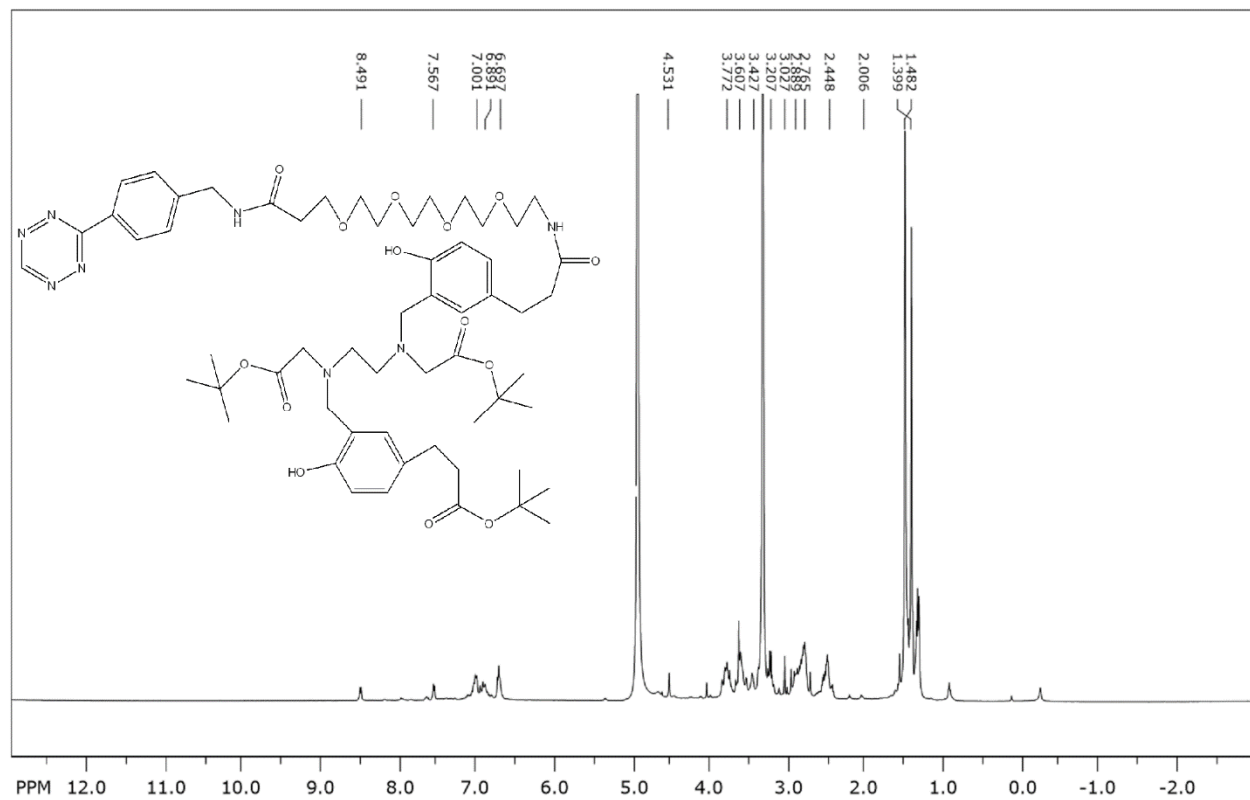
- Van den Bosch, S M, Rossin R, Renart Verkerk P, et al. Evaluation of strained alkynes for Cu-free click reaction in live mice. *Nucl Med Biol.* 2013;40(3):415-423.
- Van Swieten PF, Leeuwenburgh MA, Kessler BM, Overkleeft HS. Bioorthogonal organic chemistry in living cells: Novel strategies for labeling biomolecules. *Org Biomol Chem.* 2005;3(1):20-27.
- Vugts DJ, Vervoort A, Stigter-van Walsum M, et al. Synthesis of phosphine and Antibody–Azide probes for in vivo Staudinger ligation in a pretargeted imaging and therapy approach. *Bioconjugate Chem.* 2011;22(10):2072-2081.
- Wadas TJ, Wong EH, Weisman GR, Anderson CJ. Coordinating radiometals of copper, gallium, indium, yttrium, and zirconium for PET and SPECT imaging of disease. *Chem Rev.* 2010;110(5):2858-2902.
- Zanzonico P. Positron emission tomography: A review of basic principles, scanner design and performance, and current systems. *Semin Nucl Med.* 2004;34(2):87-111.
- Zeglis BM, Sevak KK, Reiner T, et al. A pretargeted PET imaging strategy based on bioorthogonal Diels-Alder click chemistry. *Journal of Nuclear Medicine.* 2013;54(8):1389-1396.
- Ziegler SI. Positron emission tomography: Principles, technology, and recent developments. *Nuclear Physics A.* 2005;752:679-687.

11. Appendix

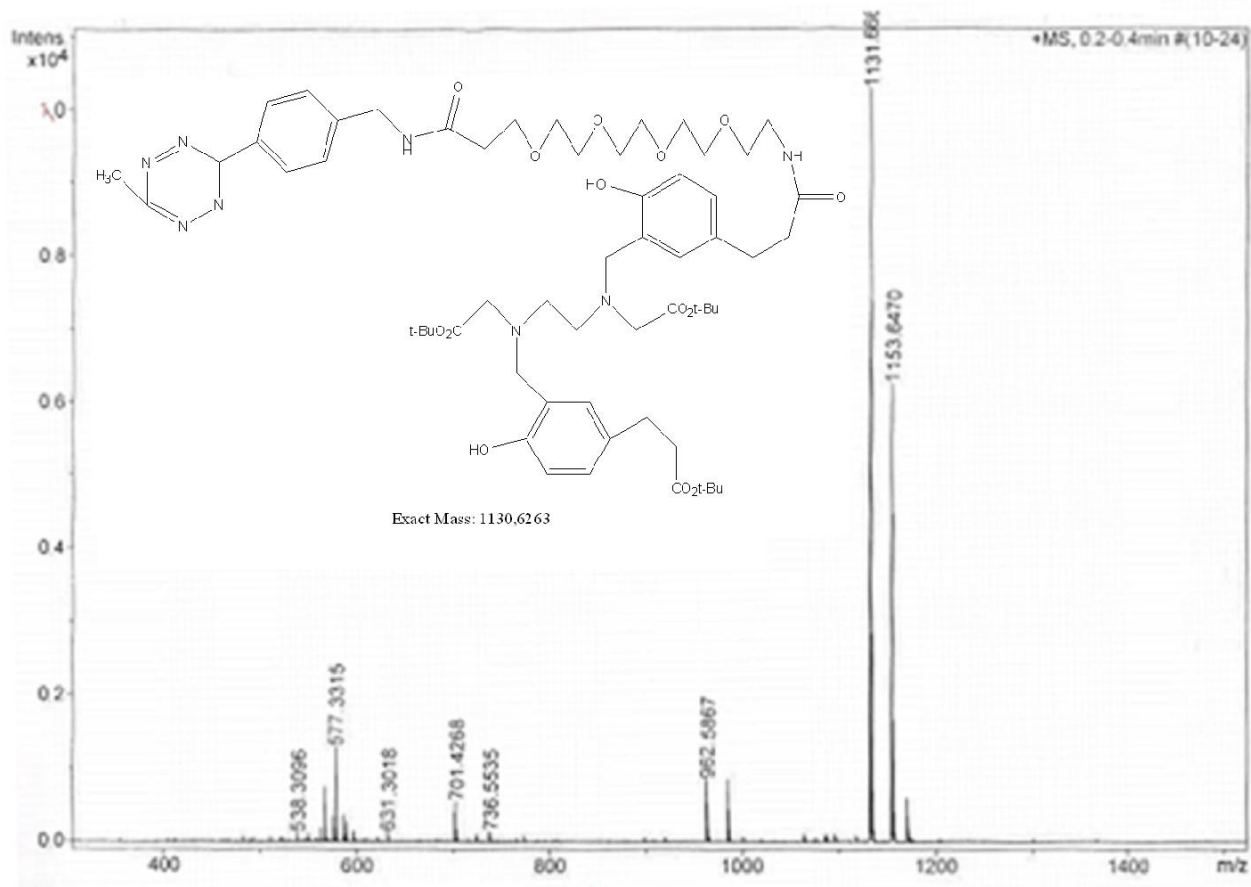
Appendix 1. MS-spectrum of tert-butyl protected HBED-CC-tetrazine-PEG4-amine (**3a**).



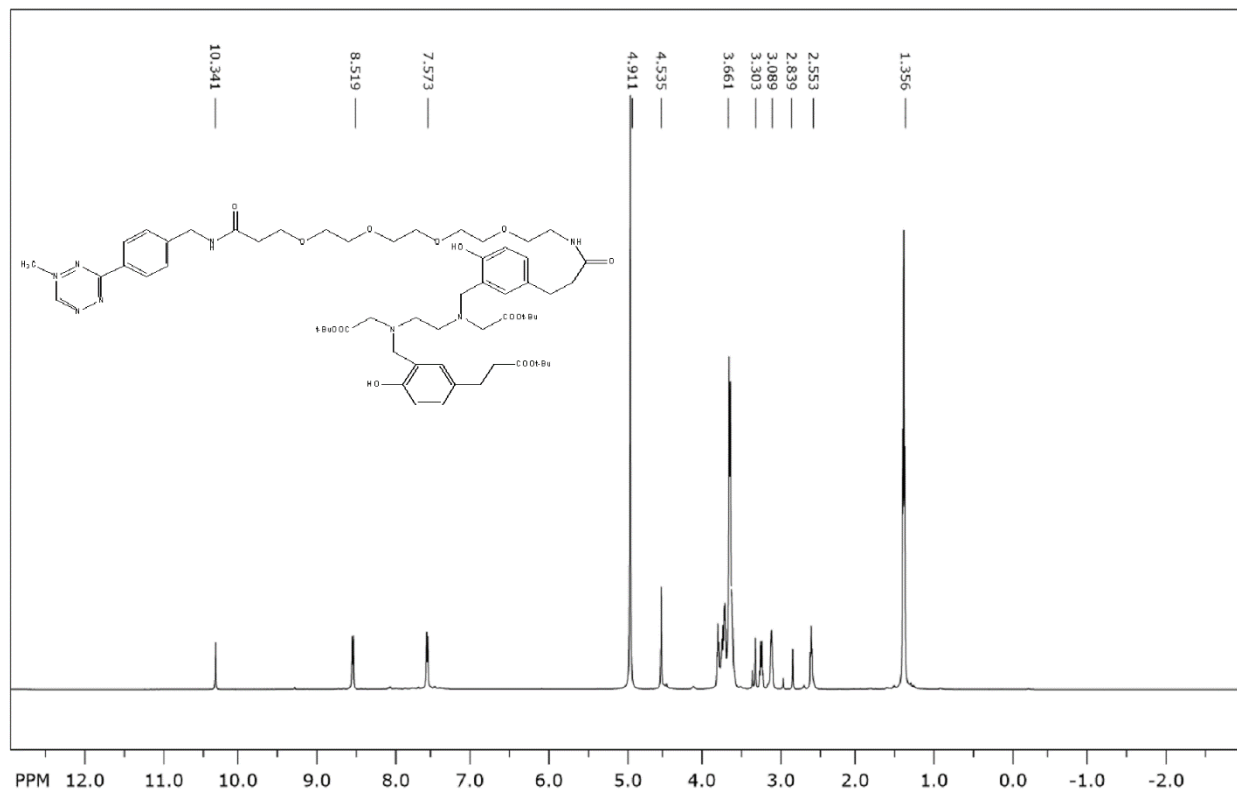
Appendix 2. $^1\text{H-NMR}$ -spectrum of tert-butyl protected HBED-CC-tetrazine-PEG4-amine (**3a**).



Appendix 3. MS-spectrum of tert-butyl protected HBED-CC-tetrazine-PEG4-amine with methyl group (**3b**).



Appendix 4. ^1H NMR-spectrum of tert-butyl protected HBED-CC-tetrazine-PEG4-amine with methyl group (**3b**).



Appendix 5. MS-spectrum of deprotected HBED-CC-tetrazine-PEG4 with methyl (**4b**).

